Joint Power and Blocklength Optimization for URLLC in a Factory Automation Scenario

Hong Ren, Cunhua Pan, Yansha Deng, *Member, IEEE*, Maged Elkashlan, and Arumugam Nallanathan, *Fellow, IEEE*

***Abstract*— Ultra-reliable and low-latency communication (URLLC) is one of three pillar applications defined in the fifth generation new radio (5G NR), and its research is still in its infancy due to the difficulties in guaranteeing extremely high reliability (say 10^{-9} packet loss probability) and low latency (say 1 ms) simultaneously. In URLLC, short packet transmission is adopted to reduce latency, such that conventional Shannon's capacity formula is no longer applicable, and the achievable data rate in finite blocklength becomes a complex expression with respect to the decoding error probability and the blocklength. To provide URLLC service in a factory automation scenario, we consider that the central controller transmits different packets to a robot and an actuator, where the actuator is located far from the controller, and the robot can move between the controller and the actuator. In this scenario, we consider four fundamental downlink transmission schemes, including orthogonal multiple access (OMA), non-orthogonal multiple access (NOMA), relay-assisted, and cooperative NOMA (C-NOMA) schemes. For all these transmission schemes, we aim for jointly optimizing the blocklength and power allocation to minimize the decoding error probability of the actuator subject to the reliability requirement of the robot, the total energy constraints, as well as the latency constraints. We further develop low-complexity algorithms to address the optimization problems for each transmission scheme. For the general case with more than two devices, we also develop a low-complexity efficient algorithm for the OMA scheme. Our results show that the relay-assisted transmission significantly outperforms the OMA scheme, while the NOMA scheme performs well when the blocklength is very limited. We further show that the relay-assisted transmission has superior performance over the C-NOMA scheme due to larger feasible region of the former scheme.**

***Index Terms*— URLLC, mission-critical IoT, IIoT, 5G NR, MTC.**

I. Introduction

THE fifth-generation (5G) networks are envisaged to support three pillar use cases: enhanced mobile broadband (eMBB), massive machine type communication (mMTC), and *mission-critical* internet of things (IoT) [1]. Extensive research has focused on eMBB and mMTC, but the research on mission-critical IoT is still in its infancy [2]–[6]. The applications of mission-critical tasks include factory automation (FA), autonomous driving, remote surgery, smart grid automation, unmanned aerial vehicles (UAVs) control information delivery [7], which require ultra reliable and low latency communication (URLLC) [8]–[10]. For example, in Industrial 4.0 [11], wired connection will be replaced by wireless transmission to enhance the flexibility and reduce the infrastructure cost. This change imposes challenging requirements on the wireless transmission in terms of latency and reliability [12]. For mission-critical tasks in FA, the transmission duration is expected to be lower than 100 μs to allow processing delays during queuing, scheduling, backhaul transmission, and propagation [13], while guaranteeing the packet error probability of 10^{-9}.

In conventional human-to-human (H2H) communications, the transmission delay is relatively long (say 20-30 ms) and the packet size is large (say 1500 bytes), thus Shannon's capacity can be served as a tight upper bound of the achievable data rate due to the law of large numbers [14]. In contrast, in URLLC, the packet size should be extremely low (say 20 bytes) to support the low-latency transmission [13]. In this case, Shannon's capacity formula is no longer applicable as the law of large numbers is not valid. Thus, the achievable data rate under short blocklength needs to be retreated. In [15], the achievable data rate in finite blocklength regime has been derived as a complicated function of the signal-to-noise (SNR), the blocklength, and the decoding error probability.

Recently, extensive research attention has been devoted to the short packet transmission (SPT) design [16]–[26]. In particular, the frame structure is designed in [16] for SPT, where their results showed that it is beneficial to group multiple messages from some users into a single packet based on approximations from finite blocklength information theory. In [17], She *et al.* studied the network available range maximization problem by dynamically selecting the transmission modes between device-to-device (D2D) and cellular links. The non-asymptotic upper and lower bounds on the coding rate for SPT over a Rician memoryless block-fading channel were derived in [18] under a given packet error probability requirement. The overall error probability of relay-assisted transmission under finite blocklength was derived in [19] under the assumption of perfect channel state information (CSI). They further extended this model to the quasi-static Rayleigh

Manuscript received October 31, 2018; revised April 18, 2019 and September 23, 2019; accepted November 28, 2019. Date of publication December 16, 2019; date of current version March 10, 2020. This article was presented in part at the IEEE ICC 2019. The associate editor coordinating the review of this article and approving it for publication was M. Payaró. *(Corresponding author: Cunhua Pan.)*

H. Ren, C. Pan, M. Elkashlan, and A. Nallanathan are with the School of Electronic Engineering and Computer Science, Queen Mary University of London, London E1 4NS, U.K. (e-mail: h.ren@qmul.ac.uk; c.pan@qmul.ac.uk; maged.elkashlan@qmul.ac.uk; a.nallanathan@qmul.ac.uk).

Y. Deng is with the Department of Informatics, King's College London, London WC2R 2LS, U.K. (e-mail: yansha.deng@kcl.ac.uk).

Color versions of one or more of the figures in this article are available online at http://ieeexplore.ieee.org.

Digital Object Identifier 10.1109/TWC.2019.2957745

channels where only the average CSI is available at the source in [20], as well as to the two-way amplify-and-forward relay network in [21]. Recently, the delay and decoding error probability were analyzed in [22] for simultaneous wireless information and power transfer (SWIPT) relay-assisted system, where the relay first harvests energy from the source and then uses the harvested energy to forward the source's information to the destination node.

The aforementioned studies [16]–[22] mainly focused on the performance analysis of finite blocklength transmission. In order to design a practical URLLC system, it is imperative to intelligently optimize the resource allocation including blocklength and power allocation under the given error probability and latency requirements. Unfortunately, the achievable coding rate expression is neither convex nor concave with respect to the blocklength and the transmit power, which brings the difficulty in obtaining the globally optimal solution [5]. This motivates the recent studies in resource allocation for the SPT in [23]–[27]. Specifically, the average throughput and the max-min throughput optimization under the latency constraint was solved via the exhaustive search method with high complexity in [23]. Sun *et al.* in [24] considered the SPT for a two-user downlink non-orthogonal multiple access (NOMA) system, with an aim to maximize the throughput of user 1 subject to the throughput requirements for user 2. Note that the decoding error probability requirement has not been considered in [23] and [24], and the throughput is less important in URRLC as only control signals or measurement data with small packet size are transmitted in URLLC. In [25], She *et al.* jointly optimized the uplink and downlink transmission blocklengths to minimize the required total bandiwidth based on statistical channel state information (CSI). However, the optimization is based on the simplified expression of the rate for SPT, which cannot accurately characterize the relationship between the decoding error probability and blocklength. In addition, several approximations are involved in the derivation of the decoding error probability for each user due to the fact that only statistical CSI is available. Most recently, Hu *et al.* [26] considered SWIPT in relay-assisted URLLC systems, where the SWIPT parameters and blocklength are jointly optimized to maximize the reliability performance. However, the decoding error probability at the relay cannot be guaranteed and the power is assumed to be fixed in [26]. Most recently, in [27] we jointly optimize the blocklength and unmanned aerial vehicle's (UAV's) location to minimize the decoding error probability while guaranteeing the latency requirement and decoding error probability target. However, the power allocation was not considered. Furthermore, the optimization over UAV's location is obtained by observing the curve of the second-order derivative of the objective function over location variable without strict proof.

In this paper, we consider a typical mission-critical scenario (i.e., a FA scenario), where the central controller needs to transmit a certain amount of different data to two devices within a given transmission time and under a very low packet error probability. One device named actuator is located far away from the controller, while the other device named robot can move between the controller and the actuator. We consider four fundamental transmission schemes, namely, orthogonal multiple access (OMA), NOMA, relay-assisted transmission and cooperative NOMA (C-NOMA). In this scenario, we aim for jointly optimizing the blocklength and the transmit power of these two devices to minimize the decoding error probability for the actuator while guaranteeing the decoding error probability for the robot, taking into account the energy and blocklength constraints, which were not considered in [24]–[26] and new methods needs to be developed. The main contributions of this paper are summarized as follows:

1) For the OMA scheme, we first prove that both the decoding error probability and energy constraints hold with equality at the optimal point, and then propose a novel iterative algorithm to obtain tight lower and upper bounds of the blocklength to reduce the search complexity. A low-complexity algorithm is proposed to find the globally optimal solution of transmit power. For the case of more than two devices, we also develop a novel low-complexity algorithms to find the suboptimal solution of the optimization problem.
2) For the NOMA scheme, the search set of blocklength is first derived to reduce the search complexity. In contrast to the OMA case, the decoding error probability function for each given blocklength in the NOMA case is non-continuous with respect to the transmit power, which complicates the optimization problem. Fortunately, we rigorously proved that the decoding error probability holds with equality at the optimal point, such that the one-dimensional line search algorithm can be used to find the optimal solution. We also provide a sufficient condition when the decoding error probability function is a convex function, which facilitates the application of a low-complexity bisection search method.
3) For the relay-assisted scheme, we also adopt the iterative algorithm to reduce the search complexity of blocklength. Unlike the OMA and NOMA schemes, the decoding error probability constraint of relay-assisted transmission does not hold with equality. To resolve this issue, we fix the blocklength, such that the original optimization problem is reduced to a one-dimension search optimization problem.
4) For the C-NOMA scheme, we adapt the iterative algorithm to reduce the search complexity of blocklength, and then one-dimension search is proposed to find the optimal transmit power. For the special case, low-complexity bisection search method is applied.
5) To compare the performance of our proposed four transmission schemes, we perform extensive simulation results, which show that the relay-assisted scheme significantly outperforms the other three schemes for most times in terms of both the decoding error probability and the network availability. Our results demonstrate the effectiveness of relaying transmission in enhancing the reliability performance in the industrial automation scenario.

The remainder of this paper is organized as follows. In Section II, the system model and the problem formulation are provided. In Section III, the transmission scheme

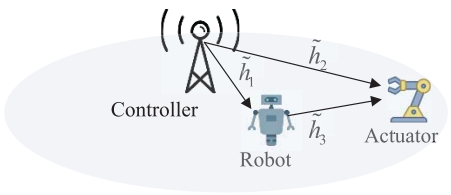

Fig. 1. Illustration of a factory automation scenario.

is presented. The general case with more than two devices is considered in Section IV. Simulation results and analysis are presented in Section V. Finally, Section VI concludes the paper.

II. System Model

A. System Model

Consider a downlink communication in one factory, where a central controller serves a robot and an actuator as shown in Fig. 1. The robot is assumed to be located in the vicinity of the controller, and the actuator is far away from the controller. Both the robot and the actuator are equipped with a single antenna. The controller needs to transmit two small packets to the two devices. The packet sizes for the actuator and the robot are assumed to be the same, and are denoted as D bits.

The transmission of these two packets is subject to a latency constraint, i.e., the transmission has to finish within M symbols or channel uses. The transmission time corresponds to $t_{\max} = MT_s$ seconds, where T_s is the symbol duration that is equal to $1/B$ with B as the system bandwidth. For the applications with URLLC requirement, short frame structure is adopted and the end-to-end delay should be kept within 1 ms [8], which is much shorter than the channel coherence time. Hence, the channels are quasi-static fading and remain constant during the whole transmission. The channel fading coefficients from the central controller to the robot and the actuator are denoted as $\tilde{h}_1$ and $\tilde{h}_2$, respectively. The channel fading coefficient between the robot and the actuator is denoted as $\tilde{h}_3$. We also assume that these channels are perfectly known at the controller, and the total energy consumption of the system should be below $\tilde{E}_{\rm tot}$ Joule. Since we have assumed that the actuator is far away from the controller, the channel power gain $\left|\tilde{h}_2\right|^2$ is very small.

B. Achievable Data Rate for a Simple Point-to-Point System

The data rate (coding rate) R of a communication system is defined as the fraction of the number of information bits to the number of transmission symbols. According to Shannon's coding theorem, the Shannon capacity is defined as the highest coding rate that there exists an encoder/decoder pair whose decoding error probability becomes negligible when the blocklength approaches infinity [28]. However, in URLLC, the blocklength for each frame is limited and small, in this case, the decoding error probability at the receiver cannot be ignored.

In URLLC scenarios, the required transmission delay is much shorter than the channel coherence time, thus the channel is quasi-static. According to the results in [29], for a simple point-to-point communication system transmitting over a quasi-static Rayleigh fading channel, the channel dispersion is zero and the achievable data rate converges to the outage capacity as the blocklength increases. However, the closed-form expression of the outage capacity for short-packet transmission is unavailable. In [15], the normal approximation was adopted to approximate the coding rate R at finite blocklength, which is given by

$$R \approx \log_2(1+\gamma) - \sqrt{\frac{V}{m}}\frac{Q^{-1}(\varepsilon)}{\ln 2}, \tag{1}$$

where m is the channel blocklength, ε is the decoding error probability, γ denotes the signal-to-noise ratio (SNR) at the receiver, $Q^{-1}(\cdot)$ is the inverse function $Q(x) = \frac{1}{\sqrt{2\pi}}\int_x^\infty e^{-\frac{t^2}{2}}dt$, and V is given by $V = 1-(1+\gamma)^{-2}$. As shown in the numerical results in [29], this approximation is very accurate when m is larger than 50, which is the case in our simulations. From (1), the decoding error probability can be obtained as follows:

$$\varepsilon = Q\left(f(\gamma, m, D)\right), \tag{2}$$

where $f(\gamma, m, D) = \ln 2\sqrt{\frac{m}{V}}\left(\log_2(1+\gamma) - \frac{D}{m}\right)$. In the following, we aim to jointly optimize the transmission blocklength and power to minimize the decoding error probability for four different transmission schemes.

III. Transmission Schemes

In this section, we aim for designing efficient resource allocation algorithms to minimize the decoding error probability of the actuator under three sets of constraints: 1) the packets for robot and actuator need to be transmitted within M symbols; 2) the robot should satisfy its reliability requirement; 3) the total consumed energy should be kept within $\tilde{E}_{\rm tot}$. The OMA, NOMA, relay-assisted transmission, and C-NOMA transmission schemes are studied in the following subsections.

A. OMA Transmission

The OMA scheme is the simplest transmission scheme, where the controller serves the robot and the actuator in two different orthogonal channel uses or blocklengths. In detail, the controller transmits signal x_1 to the robot with m_1 blocklength. Due to this orthogonal property, the received signal at the robot can be represented as

$$y_1 = \sqrt{p_1}\tilde{h}_1 x_1 + n_1, \tag{3}$$

where p_1 is the transmit power of the robot, n_1 is the zero-mean additive complex white Gaussian noise (AWGN) with variance σ_1^2, x_1 carries information knowledge for the robot with packet size D. Hence, the coding rate at the robot is given by D/m_1.

From (3), the received signal to noise ratio (SNR) at the robot is given by

$$\gamma_1 = p_1 h_1, \tag{4}$$

where $h_1 = |\tilde{h}_1|^2/\sigma_1^2$ denotes the normalized channel gain from the controller to the robot. Then, according to (2), the decoding error probability of x_1 at the robot is given by

$$\varepsilon_1 = Q\left(f\left(\gamma_1, m_1, D\right)\right). \tag{5}$$

The controller transmits signal x_2 to the actuator with blocklength equal to m_2. The corresponding error probability at the actuator is derived as

$$\varepsilon_2 = Q\left(f\left(\gamma_2, m_2, D\right)\right), \tag{6}$$

where $\gamma_2 = p_2 h_2$ with p_2 as the transmit power of the actuator and $h_2 = |\tilde{h}_2|^2/\sigma_2^2$ as the normalized channel gain for the actuator. Without loss of generality (w.l.o.g.), we assume that in this paper the robot has higher normalized channel gain than the actuator, i.e., $h_1 > h_2$.

The resource allocation problem for the OMA transmission can be formulated as:

$$\min_{\{m_1, m_2, p_1, p_2\}} \quad \varepsilon_2 \tag{7a}$$

$$\text{s.t. } \varepsilon_1 \le \varepsilon_1^{\max}, \tag{7b}$$

$$m_1 p_1 + m_2 p_2 \le E_{\text{tot}}, \tag{7c}$$

$$m_1 + m_2 \le M, \tag{7d}$$

$$m_1, m_2 \in \mathbb{Z}, \tag{7e}$$

where constraint in (7b) is the decoding error probability requirement of the robot, constraint (7c) ensures the system total energy consumption is within a budget $\tilde{E}_{\text{tot}} = E_{\text{tot}} T_s$, (7d) is the constraint on the latency constraint, and constraint (7e) ensures that the blocklength for each transmission phase is integer with $\mathbb{Z}$ denoting the positive integer set. The maximum decoding error probability $\varepsilon_1^{\max}$ is assumed to be much less than 0.1 to ensure the stringent reliability requirement, and this assumption holds for the remaining transmission schemes. As a result, ε_1 should be smaller than 0.1. Then, the inequality $\frac{D}{m_1} < \log_2(1+\gamma_1)$ should hold.

To solve the optimization problem in (7), we first provide the following lemma.

Lemma 1: Constraints (7b) and (7c) hold with equality at the optimum solution.

Proof: Please see Appendix A. ■

With m_1 and m_2 to be integers, the exhaustive search method can be used to find the optimal solution. To reduce the search complexity when M is large, we shorten the search range of m_1 and m_2. In the following, we aim to derive the bounds of m_1 and m_2.

1) The Upper and Lower Bounds of m_1 and m_2: Since $\varepsilon_1^{\max}$ is assumed to be a very small value that is much smaller than 10^{-1}, a necessary condition for constraint (7b) to hold is that $\log_2(1+p_1 h_1) > D/m_1$, [1] which leads to

$$p_1 > \left(2^{\frac{D}{m_1}} - 1\right)/h_1. \tag{8}$$

[1]This can be proved as follows: $\varepsilon_1 = Q\left(f\left(\gamma_1, m_1, D\right)\right) < \varepsilon_1^{\max} < 0.5 = Q(0)$. Since Q-function is a decreasing function, we have $f\left(\gamma_1, m_1, D\right) > 0$. By substituting the expression of $f\left(\gamma_1, m_1, D\right)$, the proof is complete.

On the other hand, based on the energy constraint (7c), we have: $p_1 < E_{\text{tot}}/m_1$. Thus, the blocklength allocation of the robot m_1 should satisfy the following inequality:

$$E_{\text{tot}} > \frac{m_1}{h_1}\left(2^{\frac{D}{m_1}} - 1\right) \triangleq g(m_1). \tag{9}$$

To investigate the properties of $g(m_1)$, the first-order and second-order derivatives of function $g(m_1)$ w.r.t. m_1 are give by

$$g'(m_1) = 2^{\frac{D}{m_1}} - 1 - \ln 2 \cdot \frac{D}{m_1} 2^{\frac{D}{m_1}}, \tag{10}$$

$$g''(m_1) = (\ln 2)^2 \cdot \frac{D^2}{m_1^3} 2^{\frac{D}{m_1}} \ge 0. \tag{11}$$

Thus, $g'(m_1)$ is a monotonically increasing function of m_1, and we have

$$g'(m_1) \le \lim_{m_1 \to +\infty} g'(m_1) = 0. \tag{12}$$

Hence, function $g(m_1)$ is a monotonically decreasing function of m_1. Then, we can find the lower bound of m_1 that satisfies the inequality (9) which is denoted as $m_1^{\text{lb}(0)}$, and m_1 should be no smaller than $m_1^{\text{lb}(0)}$, i.e., $m_1 \ge m_1^{\text{lb}(0)}$. Similarly, for practical applications, the decoding error probability of the actuator ε_2 should be very small, e.g., much lower than 0.5. In this case, the inequality $\log_2(1+p_2 h_2) > D/m_2$ should hold, which leads to

$$p_2 > \left(2^{\frac{D}{m_2}} - 1\right)/h_2. \tag{13}$$

By using the inequality $m_2 \le M - m_1^{\text{lb}(0)}$, we have

$$m_2 p_2 \ge \frac{m_2}{h_2}\left(2^{\frac{D}{m_2}} - 1\right) \tag{14}$$

$$\ge \frac{M - m_1^{\text{lb}(0)}}{h_2}\left(2^{\frac{D}{M - m_1^{\text{lb}(0)}}} - 1\right) \triangleq A^{(0)}. \tag{15}$$

By using constraint (7c), we have

$$E_{\text{tot}} - A^{(0)} > \frac{m_1}{h_1}\left(2^{\frac{D}{m_1}} - 1\right). \tag{16}$$

By using (16), the updated lower bound of m_1 can be obtained, and denoted as $m_1^{\text{lb}(1)}$. Similar to (14), we can obtain $A^{(1)}$ by substituting $m_1^{\text{lb}(1)}$ into $m_1^{\text{lb}(0)}$, and the lower bound of m_1 can be obtained by using (16), where $A^{(0)}$ is replaced by $A^{(1)}$, and the updated lower bound is denoted as $m_1^{\text{lb}(2)}$. Repeat the above procedure until $m_1^{\text{lb}(n)} = m_1^{\text{lb}(n-1)}$ or $m_1^{\text{lb}(n)} = M - m_2^{\text{lb}(0)}$. Then, denote the final lower bound of m_1 as m_1^{lb}.

This procedure is proved to converge as follows. By using $A^{(0)} \ge 0$ and comparing (9) and (16), we can obtain $m_1^{\text{lb}(1)} \ge m_1^{\text{lb}(0)}$, and thus $A^{(1)} \ge A^{(0)}$, which leads to $m_1^{\text{lb}(2)} \ge m_1^{\text{lb}(1)}$. Hence, the sequence of the lower bound $m_1^{\text{lb(n)}}$ is monotonically increasing. Furthermore, the sequence is upper bounded by $M - m_2^{\text{lb}(0)}$. As a result, the sequence generated by the above iterative procedure is guaranteed to converge.

By using the similar iterative procedure, we can also obtain the lower bound of m_2, which is denoted as m_2^{lb}. As a result, the search region of m_1 is given by $m_1^{\text{lb}} \le m_1 \le (M - m_2^{\text{lb}}) \triangleq m_1^{\text{ub}}$.

For each given m_1, we need to find the search range of m_2, which is detailed as follows. The optimal p_1 can be obtained by solving the equation $\varepsilon_1 = \varepsilon_1^{\max}$ with given m_1, which is denoted as p_1^*. The solution can be readily obtained by using the bisection search method due to the fact that $\varepsilon_1(p_1)$ is a monotonically decreasing function of p_1. Then, we have

$$E_{\rm tot} - m_1 p_1^* = m_2 p_2 \geq \frac{m_2}{h_2}\left(2^{\frac{D}{m_2}} - 1\right). \tag{17}$$

Hence, the lower bound of m_2 with given m_1 (denoted as $m_2^{\rm lb}(m_1)$) can be obtained from (17), which is the minimum integer that satisfies (17). Obviously, the upper bound of m_2 with given m_1 is $M - m_1$. Hence, the search region of m_2 is given by $m_2^{\rm lb}(m_1) \leq m_2 \leq (M - m_1)$.

Algorithm 1 Algorithm for Problem (7)

Input : $h_1, h_2, D, M, \varepsilon_1^{\max}, E_{\rm tot}$
Output: $p_1^\star, p_2^\star, m_1^\star, m_2^\star$

Apply the iterative procedure to calculate $m_1^{\rm lb}, m_1^{\rm ub}$ and $m_2^{\rm lb}$;
for $m_1 = m_1^{\rm lb} : m_1^{\rm ub}$ **do**
  Set $p_1 = E_{\rm tot}/m_1$, and calculate the value of ε_1.
  if $\varepsilon_1 > \varepsilon_1^{\max}$ **then**
    The current m_1 is not feasible, and return to the next m_1;
  else
    Use (17) to find the lower bound of m_2, denoted as $m_2^{\rm lb}(m_1)$. Apply the bisection search method to find the value of p_1 such that $\varepsilon_1 = \varepsilon_1^{\max}$;
    for $m_2 = m_2^{\rm lb}(m_1) : M - m_1$ **do**
      Calculate $p_2 = (E_{\rm tot} - m_1 p_1)/m_2$, and the value of ε_2, denoted as $\varepsilon_2(m_1, m_2)$.
    end
    Given m_1, find the blocklength m_2 with the minimum value of $\varepsilon_2(m_1, m_2)$:

$$m_2^{\#}\Big|_{m_1} = \mathop{\arg\min}_{m_2^{\rm lb} \leq m_2 \leq M - m_1} \varepsilon_2(m_1, m_2).$$

  end
end
Return

$$m_1^\star = \mathop{\arg\min}_{m_1^{\rm lb} \leq m_1 \leq m_1^{\rm ub}} \varepsilon_2\left(m_1, m_2^{\#}\Big|_{m_1}\right), m_2^\star = m_2^{\#}\Big|_{m_1^\star}$$

and the corresponding $p_1^\star$ and $p_2^\star$.

2) Algorithm to Solve Problem (7): Based on the above analysis, the algorithm to solve Problem (7) is given in Algorithm 1. The main idea can be summarized as follows. For each given integer value of m_1 that satisfies $m_1^{\rm lb} \leq m_1 \leq m_1^{\rm ub}$, we calculate the value of ε_1 when p_1 is set as $E_{\rm tot}/m_1$. If $\varepsilon_1 > \varepsilon_1^{\max}$, then the value of m_1 is not feasible, and we increase the value of m_1 by one and continue to check the updated m_1. Otherwise, we apply the bisection search method to find the value of p_1 such that $\varepsilon_1 = \varepsilon_1^{\max}$ due to the monotonically decreasing property of decoding error probability ε_1 w.r.t. p_1 [24]. By using Lemma 1, we have $m_2 p_2 = E_{\rm tot} - m_1 p_1$. The search range of m_2 is given by $m_2^{\rm lb}(m_1) \leq m_2 \leq M - m_1$. For each given m_2, the corresponding p_2 is given by $p_2 = (E_{\rm tot} - m_1 p_1)/m_2$, and we can calculate the value of ε_2. For each feasible m_1, we can find the optimal solutions for m_2 and p_2 that yield the minimum value of ε_2, respectively. At last, we check all feasible m_1 in the range of $m_1^{\rm lb} \leq m_1 \leq m_1^{\rm ub}$, and choose the final globally optimal solution.

3) Special Case of Problem (7): In steps 8-10 of Algorithm 1, one has to calculate the value of ε_2 for each m_2, which may incur high complexity. In this subsection, we consider one special case when the SNR value γ is very high, i.e., $\gamma \gg 1$. In this case, V in (2) can be approximated as one, i.e., $V \approx 1$. [2] The optimization problem in this special case can be efficiently solved. Specifically, the decoding error probability in (2) can be approximated as

$$\tilde{\varepsilon} = Q\left(\tilde{f}(\gamma, m, D)\right), \tag{18}$$

where $\tilde{f}(\gamma, m, D) = \ln 2\sqrt{m}\left(\log_2(1+\gamma) - \frac{D}{m}\right)$.

For given m_1 and p_1, the product of m_2 and p_2 should satisfy $m_2 p_2 = E_{\rm tot} - m_1 p_1 \triangleq E_2$ according to Lemma 1. Then, the original problem defined in (7) can be transformed to the following optimization problem:

$$\min_{m_2^{\rm lb} \leq m_2 \leq M - m_1, m_2 \in \mathbb{Z}} Q\left(\tilde{f}(\gamma_2, m_2, D)\right). \tag{19}$$

Since Q-function is a decreasing function, the above problem is equivalent to the following problem by substituting $p_2 = E_2/m_2$ into it as

$$\max_{m_2^{\rm lb} \leq m_2 \leq M - m_1, m_2 \in \mathbb{Z}} \ln 2\sqrt{m_2}\left(\log_2\left(1 + \frac{E_2 h_2}{m_2}\right) - \frac{D}{m_2}\right). \tag{20}$$

To solve the above problem, we first relax the integer variable m_2 to a continuous variable, and define

$$\tilde{g}(m_2) \triangleq \sqrt{m_2}\left(\log_2\left(1 + \frac{E_2 h_2}{m_2}\right) - \frac{D}{m_2}\right). \tag{21}$$

In the following theorem, we provide a sufficient condition for $\tilde{g}(m_2)$ to be a concave function.

Theorem 1: $\tilde{g}(m_2)$ is a concave function when $\frac{E_2 h_2}{M - m_1} \geq e - 1$, where e is the natural constant.

Proof: Please see Appendix B. ∎

When the condition in Theorem 1 is satisfied, Problem (20) is a convex optimization problem. If $\tilde{g}'(m_2^{\rm lb}) \leq 0$, the optimal m_2 is given by $m_2 = m_2^{\rm lb}$. If $\tilde{g}'(M - m_1) \geq 0$, the optimal m_2 is $m_2 = M - m_1$. Otherwise, the optimal m_2^* satisfies $\tilde{g}'(m_2) = 0$, and the low-complexity bisection search method can be used to find m_2^*. The final optimal integer m_2 is the one with lower objective value for its two neighbor integers, i.e., $\lfloor m_2^* \rfloor$ and $\lfloor m_2^* \rfloor + 1$.

B. NOMA Transmission

In NOMA transmission, superposition coding is employed at the controller so that the controller can transmit signals to the two devices simultaneously with different power levels. The controller allocates higher transmit power to the user with lower channel gains and lower power to the one with

[2] In general, when $\gamma > 20$ dB, the value of V is larger than 0.99, which can be approximated as one.

higher channel gains. On the one hand, the robot decodes the actuator's signal first. If decoding correctly, the robot will subtract the actuator's signal from its received signals and decodes its own signal. This is the so-called successive interference cancellation (SIC). Otherwise, it has to decode its own signal by treating actuator's information as interference. On the other hand, the actuator directly decodes its own signal by treating the robot's signal as interference since the controller allocates higher transmit power than the robot. To implement this scheme, it is crucial that the robot knows whether SIC is successful or not. To this end, we assume that the controller sends the actuator's channel coding information along with the robot's channel coding information to the robot through dedicated error-free channels. The channel coding information for both devices are different and the channel coding can assist in detecting whether the decoded information is correct or not. Hence, the robot knows whether the SIC is successful or not. In general, the channel coding information changes when CSI changes, which is much longer than the URLLC transmission. Hence, each channel coherence time can accommodate multiple URLLC transmissions. Then, the coding information only needs to be transmitted to the robot at the beginning of channel coherence time, which causes negligible overhead consumption.

In NOMA, the transmission blocklength for two devices is equal to M. Specifically, the received signals at the robot and the actuator are given by

$$\begin{aligned} y_1 &= \sqrt{p_1}\tilde{h}_1 x_1 + \sqrt{p_2}\tilde{h}_1 x_2 + n_1, \\ y_2 &= \sqrt{p_1}\tilde{h}_2 x_1 + \sqrt{p_2}\tilde{h}_2 x_2 + n_2, \end{aligned} \tag{22}$$

where the notations in (22) has the same meaning as those in the OMA transmission scheme. For the robot, it first decodes the actuator's signal, where the decoding signal to interference plus noise ratio (SINR) is given by

$$\gamma_2^1 = \frac{p_2 h_1}{p_1 h_1 + 1}. \tag{23}$$

Following (2), the decoding error probability of x_2 at the robot can be written as $\varepsilon_2^1 = Q\left(f\left(\gamma_2^1, M, D\right)\right)$. This equivalently indicates that the information x_2 can be accurately cancelled at the robot with probability $1-\varepsilon_2^1$. Note that this is different from the infinite blocklength case in NOMA, where perfect decoding can be achieved by the robot. If the SIC is successful, the robot decodes its signal x_1 by removing the decoded signal x_2. By using the first equality in (22), the SINR of decoding the signal x_1 is given by

$$\gamma_1 = p_1 h_1. \tag{24}$$

Thus, following (2), the decoding error probability of x_1 at the robot under perfect SIC condition is given by $\varepsilon_1 = Q\left(f\left(\gamma_1, M, D\right)\right)$. However, if the SIC fails, the robot will decode its information x_1 while treating x_2 as interference, and the corresponding SINR is given by

$$\hat{\gamma}_1 = \frac{p_1 h_1}{p_2 h_1 + 1}. \tag{25}$$

Thus, the decoding error probability of x_1 at the robot is given by $\hat{\varepsilon}_1 = Q\left(f\left(\hat{\gamma}_1, M, D\right)\right)$. Based on the above discussion, the decoding error probability of x_1 at the robot is Bernoulli-distributed. With probability $1-\varepsilon_2^1$, the decoding error probability is equal to ε_1, and with probability ε_2^1, it is equal to $\hat{\varepsilon}_1$. Hence, the average decoding error probability of x_1 at the robot is formulated as

$$\bar{\varepsilon}_1 = \varepsilon_1(1-\varepsilon_2^1) + \hat{\varepsilon}_1\varepsilon_2^1. \tag{26}$$

Recall that the actuator directly decodes its own signal by treating the signal from the robot as interference, and its SINR is given by

$$\gamma_2 = \frac{p_2 h_2}{p_1 h_2 + 1}. \tag{27}$$

The corresponding decoding error probability is given by $\varepsilon_2 = Q\left(f\left(\gamma_2, M, D\right)\right)$.

Now, we can formulate the optimization problem under NOMA transmission as:

$$\min_{\{p_1,p_2\}} \quad \varepsilon_2 \tag{28a}$$

$$\text{s.t. } \bar{\varepsilon}_1 \le \varepsilon_1^{\max}, \tag{28b}$$

$$Mp_1 + Mp_2 \le E_{\text{tot}}, \tag{28c}$$

$$p_1 \le p_2, \tag{28d}$$

where (28d) represents that more power should be allocated to the user with weaker channel gains.

Similar to the proof of Lemma 1, we can show that the energy constraint in (28c) holds with equality at the optimum point. Then, we study the feasible range of the power allocation p_1 to facilitate the search algorithm. The expression of $\bar{\varepsilon}_1$ can be reexpressed as

$$\bar{\varepsilon}_1 = \varepsilon_1 + (\hat{\varepsilon}_1 - \varepsilon_1)\varepsilon_2^1 \ge \varepsilon_1. \tag{29}$$

By using constraints (28b) and (29), we have $\varepsilon_1 \le \varepsilon_1^{\max}$. By denoting $\bar{f}(\gamma) = f(\gamma, M, D)$, the lower bound of p_1 can be derived as

$$p_1 \ge \frac{\bar{f}^{-1}\left(Q^{-1}(\varepsilon_1^{\max})\right)}{h_1} \triangleq p_1^{\text{lb}}. \tag{30}$$

From constraint (28d), we know that $p_1 \le \frac{E_{\text{tot}}}{2M}$. To guarantee the meaningfulness of ε_2^1, the inequality $\log_2\left(1+\gamma_2^1\right) \ge D/M$ should hold. Then, we have

$$p_1 \le \frac{E_{\text{tot}} 2^{-\frac{D}{M}}}{M} - \frac{1}{h_1} + \frac{2^{-\frac{D}{M}}}{h_1}. \tag{31}$$

In addition, to guarantee the meaningfulness of ε_2, the inequality $\log_2(1+\gamma_2) \ge D/M$ should hold, which yields

$$p_1 \le \frac{E_{\text{tot}} 2^{-\frac{D}{M}}}{M} - \frac{1}{h_2} + \frac{2^{-\frac{D}{M}}}{h_2}. \tag{32}$$

Since $h_1 > h_2$, the upper bound of p_1 is given by

$$p_1 \le \min\left\{\frac{E_{\text{tot}} 2^{-\frac{D}{M}}}{M} - \frac{1}{h_2} + \frac{2^{-\frac{D}{M}}}{h_2}, \frac{E_{\text{tot}}}{2M}\right\} \triangleq p_1^{\text{ub}}. \tag{33}$$

To further reduce the search complexity, in the following theorem, we prove that constraint (28b) holds with equality at the optimum point.

Theorem 2: Constraint (28b) holds with equality at the optimum solution.

Proof: Please see Appendix C. ■

Based on Theorem 2, we can readily know that the one-dimensional line search algorithm can be used to find the optimal $p_1^\star$.

C. Relay-Assisted Transmission

In this scheme, the robot acts as a relay that assists the transmission for actuator, where decode-and-forward (DF) relay is assumed at the robot. The packet ID is inserted in the packet head for each device to differentiate their corresponding data information. The whole blocklength is divided into two phases, the broadcast phase with blocklength m_1 and the relay phase with blocklength m_2, which satisfy the constraint of $m_1 + m_2 \leq M$.

In the first phase, the controller broadcasts a large packet that is a combination of two packets to both devices, where the combined packet size is $2D$. The received signals at both devices are given by

$$\begin{aligned} y_{1,1} &= \sqrt{p_s}\tilde{h}_1\tilde{x}_1 + n_1, \\ y_{1,2} &= \sqrt{p_s}\tilde{h}_2\tilde{x}_1 + n_2, \end{aligned} \tag{34}$$

where p_s denotes the power allocated to the combined packet, $\tilde{x}_1$ carries the data information of the combined packet with coding rate $2D/m_1$. Then, the SNR of the robot to decode the combined packet is given by $\gamma_1 = p_s h_1$, and the decoding error probability at the robot is given by $\varepsilon_1 = Q\left(f\left(\gamma_1, m_1, 2D\right)\right)$.

Since the robot acts as a relay based on the DF mode, if the robot successfully decodes the combined packet, it will forward the actuator's packet to the actuator with coding rate D/m_2 in the second phase, and the received signal at the actuator is given by

$$y_{2,2} = \sqrt{p_r}\tilde{h}_3 x_2 + n_3, \tag{35}$$

where p_r is the transmit power at the actuator. The received SNR is $\gamma_2 = p_r h_3$, where h_3 is the normalized channel gain given by $h_3 = |\tilde{h}_3|^2/\sigma_2^2$. The error probability is given by $\varepsilon_2 = Q\left(f\left(\gamma_2, m_2, D\right)\right)$.

There is a possibility that the actuator cannot decode its packet due to the following two reasons: 1) the robot is not able to correctly decode the combined packet and will not forward anything to the actuator with probability ε_1; and 2) the robot correctly decodes the combined packet and forwards the packet to the actuator with probability $1 - \varepsilon_1$, but with probability ε_2, the actuator fails to decode the packet. In this case the actuator will have to decode the combined packet by using the received signal from the first phase, i.e., $y_{1,2}$. The achieved SNR of the actuator for decoding the combined packet is given by $\hat{\gamma}_2 = p_s h_2$, and the corresponding decoding error probability is given by $\hat{\varepsilon}_2 = Q\left(f\left(\hat{\gamma}_2, m_1, 2D\right)\right)$.

As a result, the expected error probability of the actuator decoding its packet in the relay-assisted transmission scheme is given by

$$\bar{\varepsilon}_2 = \left(\left(1 - \varepsilon_1\right)\varepsilon_2 + \varepsilon_1\right)\hat{\varepsilon}_2. \tag{36}$$

Then, the resource allocation problem is formulated as

$$\min_{\{m_1, m_2, p_s, p_r\}} \quad \bar{\varepsilon}_2 \tag{37a}$$

$$\text{s.t. } \varepsilon_1 \leq \varepsilon_1^{\max}, \tag{37b}$$

$$m_1 p_s + m_2 p_r \leq E_{\text{tot}}, \tag{37c}$$

$$m_1 + m_2 \leq M, \tag{37d}$$

$$m_1, m_2 \in \mathbb{Z}. \tag{37e}$$

By using the contradiction method, we can easily prove that constraint (37c) holds with equality at the optimal solution. However, in contrast to the above two transmission schemes, the decoding error probability constraint (37b) may not hold with equality at the optimal solution, as the objective function may also decrease with ε_1. The algorithms proposed for the OMA and NOMA transmission schemes cannot be applied.

By using the similar iterative procedure in OMA scheme, we are able to obtain the feasible region of m_1 as $m_1^{\text{lb}} \leq m_1 \leq m_1^{\text{ub}}$. For given m_1, the search region of m_2 can also be obtained as $m_2^{\text{lb}}(m_1) \leq m_2 \leq (M - m_1)$.

In the following, we study the optimization problem of the power allocation p_s and p_r under fixed m_1 and m_2. For each given m_2, we can obtain the lower bound of p_r to make ε_2 meaningful: $p_r \geq \left(2^{D/m_2} - 1\right)/h_3 \triangleq p_r^{\text{lb}}$. Thus, the upper bound of p_s can be derived as

$$p_s \leq \frac{E_{\text{tot}}}{m_1} - \frac{m_2}{m_1} p_r^{\text{lb}} \triangleq p_s^{\text{up}}. \tag{38}$$

Hence, the feasible region of p_s is given by $p_s^{\text{lb}} \leq p_s \leq p_s^{\text{ub}}$, where p_s^{lb} is the solution to equation $\varepsilon_1(p_s) = \varepsilon_1^{\max}$ with given m_1. When p_s is given, p_r can be calculated as $p_r = (E_{\text{tot}} - m_1 p_s)/m_2$. Then, the original optimization problem reduces to a one-dimension optimization problem as

$$\min_{p_s} \quad \bar{\varepsilon}_2 \tag{39a}$$

$$\text{s.t. } p_s^{\text{lb}} \leq p_s \leq p_s^{\text{ub}}. \tag{39b}$$

The one-dimensional line search method can be used to solve Problem (39).

In summary, we provide Algorithm 2 to solve Problem (37).

D. C-NOMA Transmission

In this part, we consider the C-NOMA transmission in [30], which is a combination of the NOMA scheme and relay-assisted scheme. Specifically, in the first phase, the controller transmits two signals x_1 and x_2 to the two devices via the NOMA technique. In the second phase, the robot acts as a relay and forwards the packet to the actuator. The blocklength for these two phases are denoted by m_1 and m_2, which satisfies $m_1 + m_2 \leq M$.

Specifically, in the first phase, the received signals at the robot and the actuator are given by

$$\begin{aligned} y_{1,1} &= \sqrt{p_1}\tilde{h}_1 x_1 + \sqrt{p_2}\tilde{h}_1 x_2 + n_1, \\ y_{1,2} &= \sqrt{p_1}\tilde{h}_2 x_1 + \sqrt{p_2}\tilde{h}_2 x_2 + n_2, \end{aligned} \tag{40}$$

respectively, where p_1 and p_2 are the transmit power allocated to the robot and the actuator, x_1 and x_2 carries different information knowledge for different packets with size D.

Algorithm 2 Algorithm for Problem (37)

Input : $h_1, h_2, D, M, \varepsilon_1^{\max}, E_{\text{tot}}$

Output: $p_s^\star, p_r^\star, m_1^\star, m_2^\star$

Apply the iterative procedure to calculate $m_1^{\text{lb}}, m_1^{\text{ub}}$ and m_2^{lb};

for $m_1 = m_1^{\text{lb}} : m_1^{\text{ub}}$ **do**

  Calculate the solution to the equation $\varepsilon_1 = \varepsilon_1^{\max}$, which is denoted as p_s^{lb}. Calculate the lower bound of m_2 with given m_1, denoted as $m_2^{\text{lb}}(m_1)$.

  for $m_2 = \tilde{m}_2^{\text{lb}} : (M - m_1)$ **do**

    Calculate the upper bound of p_s as p_s^{ub} in (38), and solve Problem (39). Calculate the objective value $\bar{\varepsilon}_2(m_1, m_2)$.

  end

  Given m_1, find the blocklength m_2 with the minimum value of $\varepsilon_2(m_1, m_2)$:

$$m_2^{\#}\Big|_{m_1} = \underset{\tilde{m}_2^{\text{lb}} \le m_2 \le M - m_1}{\arg\min} \varepsilon_2(m_1, m_2).$$

end

Return

$$m_1^\star = \underset{m_1^{\text{lb}} \le m_1 \le m_1^{\text{ub}}}{\arg\min} \varepsilon_2\left(m_1, m_2^{\#}\Big|_{m_1}\right), m_2^\star = m_2^{\#}\Big|_{m_1^\star}$$

and the corresponding $p_s^\star$ and $p_r^\star$.

Hence, the coding rate for the transmission to the robot and the actuator are given by D/m_1.

By using the NOMA scheme, the SIC technique is employed at the robot side to cancel the interference from the actuator. Similar to the analysis in the NOMA scheme, the decoding error probability of x_2 at the robot is given by

$$\varepsilon_2^1 = Q\left(f\left(\gamma_2^1, m_1, D\right)\right), \tag{41}$$

where γ_2^1 is the same as that in (23). Under perfect SIC condition, the decoding error probability of x_1 at the robot is given by

$$\varepsilon_1 = Q\left(f\left(\gamma_1, m_1, D\right)\right), \tag{42}$$

where $\gamma_1 = p_1 h_1$. However, if SIC fails, the corresponding decoding error probability of x_1 at the robot is given by $\hat{\varepsilon}_1 = Q\left(f\left(\hat{\gamma}_1, m_1, D\right)\right)$, where $\hat{\gamma}_1$ is given by (25). Using the same analysis as in NOMA, the average decoding probability at the robot is given by

$$\bar{\varepsilon}_1 = \varepsilon_1(1 - \varepsilon_2^1) + \hat{\varepsilon}_1 \varepsilon_2^1. \tag{43}$$

By using the similar analysis as in the relay-assisted scheme, the decoding error probability of the actuator decoding x_2 under the C-NOMA scheme is given by

$$\bar{\varepsilon}_2 = \left(\left(1 - \varepsilon_2^1\right)\varepsilon_2 + \varepsilon_2^1\right)\hat{\varepsilon}_2, \tag{44}$$

where ε_2^1 and ε_2 are given in Subsection-III-B, and $\hat{\varepsilon}_2$ is the decoding error probability of the actuator when the actuator has to decode x_2 from the received signal in the first phase. The expression of $\hat{\varepsilon}_2$ is given by

$$\hat{\varepsilon}_2 = Q\left(f\left(\hat{\gamma}_2, m_1, D\right)\right), \tag{45}$$

where $\hat{\gamma}_2$ is given by

$$\hat{\gamma}_2 = \frac{p_2 h_2}{p_1 h_2 + 1}. \tag{46}$$

Therefore, the optimization problem of C-NOMA transmission scheme can be formulated as

$$\min_{\{m_1, m_2, p_1, p_2, p_r\}} \bar{\varepsilon}_2 \tag{47a}$$

$$\text{s.t. } \bar{\varepsilon}_1 \le \varepsilon_1^{\max}, \tag{47b}$$

$$m_1(p_1 + p_2) + m_2 p_r \le E_{\text{tot}}, \tag{47c}$$

$$m_1 + m_2 \le M, \tag{47d}$$

$$m_1, m_2 \in \mathbb{Z}, \tag{47e}$$

$$p_1 \le p_2. \tag{47f}$$

Following the similar proof as Lemma 1, we can show that constraints (47b) and (47c) hold with equality at the optimal point, thus the search method can be used to find the optimal solution of Problem (47). To reduce the search complexity, we need to find tight lower and upper bounds on m_1 and m_2.

However, unlike the previous schemes that only two power allocation variables are involved, the number of power allocation variables in C-NOMA scheme is three. This will complicate the analysis of deriving the bounds of m_1 and m_2. To deal with this difficulty, we regard the summation of $p_1 + p_2$ as a whole entity. To realize the functionality of the C-NOMA scheme, ε_1 and ε_2^1 should be very small, e.g., much lower than 0.5. Then, we have

$$p_1 \ge \frac{1}{h_1}\left(2^{\frac{D}{m_1}} - 1\right), \tag{48}$$

$$p_2 \ge \frac{1}{h_1}\left(2^{\frac{D}{m_1}} - 1\right)(1 + p_1 h_1). \tag{49}$$

By substituting (48) into the right hand side of (49), we have

$$p_2 \ge \frac{1}{h_1}\left(2^{\frac{D}{m_1}} - 1\right)2^{\frac{D}{m_1}}. \tag{50}$$

By adding (48) and (50), one can obtain

$$p_1 + p_2 \ge \frac{1}{h_1}\left(2^{\frac{2D}{m_1}} - 1\right). \tag{51}$$

To ensure that ε_2 is meaningful, we have

$$p_r \ge \frac{1}{h_3}\left(2^{\frac{D}{m_2}} - 1\right). \tag{52}$$

By using the similar iterative procedure, we can also obtain the lower bounds of m_1 and m_2, which are denoted as m_1^{lb} and m_2^{lb}, respectively. As a result, the search region of m_1 is given by $m_1^{\text{lb}} \le m_1 \le (M - m_2^{\text{lb}}) \triangleq m_1^{\text{ub}}$. For each given m_1 within the range, we need to find the search range of m_2, which is detailed as follows. Since $\varepsilon_1 < \bar{\varepsilon}_1 \le \varepsilon_1^{\max}$, the lower bound of p_1 can be obtained by solving the equation of $\varepsilon_1(p_1) = \varepsilon_1^{\max}$ for given m_1, which is denoted as p_1^{lb}. By using (49), we can obtain the lower bound of p_2 as follows:

$$p_2 \ge \frac{1}{h_1}\left(2^{\frac{D}{m_1}} - 1\right)\left(1 + p_1^{\text{lb}} h_1\right) \triangleq p_2^{\text{lb}}. \tag{53}$$

Based on (47c), we have

$$E_{\text{tot}} - m_1(p_1^{\text{lb}} + p_2^{\text{lb}}) \ge m_2 p_r \ge \frac{m_2}{h_3}\left(2^{\frac{D}{m_2}} - 1\right), \tag{54}$$

where the last inequality is due to the fact that $p_r \geq \frac{1}{h_3}\left(2^{\frac{D}{m_2}}-1\right)$ must hold to guarantee the meaningfulness of ε_2. The lower bound of m_2 under given m_1 (denoted as $m_2^{\rm lb}(m_1)$) can be obtained from (54), which is the minimum integer that satisfies (54). Obviously, the upper bound of m_2 with given m_1 is $M-m_1$. Hence, the search region of m_2 is given by $m_2^{\rm lb}(m_1) \leq m_2 \leq (M-m_1)$.

Given m_1 and m_2, we need to find the optimal p_1, p_2 and p_s. These variables are coupled and it is difficult to find the optimal solution by using the optimization method. The one-dimensional search is adopted to find the optimal solution. In particular, we first fix the value of the sum of p_1 and p_2 as t, i.e., $t=p_1+p_2$. Since constraint (47b) holds with equality at the optimal point, the optimal p_1 can be obtained by solving the equation $\bar{\varepsilon}_1(p_1)=\varepsilon_1^{\max}$ by inserting $p_2=t-p_1$ into this equation. By combining (49) and (47f), the upper bound of p_1 is obtained as $p_1 \leq \min\left(t\cdot 2^{-\frac{D}{m_1}}-\frac{1}{h_1}+\frac{1}{h_1}\cdot 2^{-\frac{D}{m_1}}, \frac{t}{2}\right) \triangleq p_1^{\rm up}$, and p_1 should be within the domain $p_1 \in (p_1^{\rm lb}, p_1^{\rm up})$. This equation has only one variable p_1 and the one-dimensional search method can be adopted to solve the equation. As constraint (47c) holds with equality, p_r can be directly obtained as $p_r=(E_{\rm tot}-tm_1)/m_2$. Calculate the objective value with given m_1, m_2, t and p_r. The remaining task is to find the tight search region t. Obviously, the lower bound of t is given by $t^{\rm lb}=p_1^{\rm lb}+p_2^{\rm lb}$. To obtain the upper bound of t, we first find the lower bound of m_2p_r, which is given by

$$m_2 p_r \geq \frac{m_2}{h_3}\left(2^{\frac{D}{m_2}}-1\right). \tag{55}$$

Then, the upper bound of t is given by

$$t \leq \frac{1}{m_1}\left(E_{\rm tot}-\frac{m_2}{h_3}\left(2^{\frac{D}{m_2}}-1\right)\right)=t^{\rm ub}. \tag{56}$$

Based on the above analysis, we provide Algorithm 3 to solve Problem (37).

Remark: It is noted that the feasible region of C-NOMA scheme is smaller than that of the relay-assisted transmission scheme. Specifically, if p_1^* and p_2^* is any one feasible solution of Problem (47), it can be readily checked that $p_s=p_1^*+p_2^*$ is also a feasible solution of Problem (37). However, if $\{p_1^*, p_2^*\}$ is not a feasible solution of Problem (47), $p_s=p_1^*+p_2^*$ may still be feasible for Problem (37). For example, by letting

$$p_2=\frac{1}{h_2}\left(2^{\frac{D}{m_1}}-1\right), p_1=\frac{1}{h_1}\left(2^{\frac{2D}{m_1}}-1\right)-\frac{1}{h_2}\left(2^{\frac{D}{m_1}}-1\right), \tag{57}$$

it can be readily checked that p_1 and p_2 do not satisfy condition (49), which is not feasible for Problem (47). However by setting $p_s=p_1+p_2$, p_s is still feasible for Problem (37). This observation means the feasible region for Problem (37) is larger than that of Problem (47).

Algorithm 3 Algorithm for Problem (47)

Input : $h_1, h_2, h_3, D, M, \varepsilon_1^{\max}, E_{\rm tot}$
Output: $p_1^\star, p_2^\star, p_r^\star, m_1^\star, m_2^\star$

Apply the iterative procedure to calculate $m_1^{\rm lb}, m_1^{\rm ub}$ and $m_2^{\rm lb}$;
for $m_1 = m_1^{\rm lb} : m_1^{\rm ub}$ **do**
  Calculate the solution to the equation $\varepsilon_1=\varepsilon_1^{\max}$, which is denoted as $p_1^{\rm lb}$. Use (53) to calculate the lower bound of p_2, denoted as $p_2^{\rm lb}$. Use (54) to find the lower bound of m_2, denoted as $m_2^{\rm lb}(m_1)$.
  if $m_2^{\rm lb}(m_1) \leq (M-m_1)$ **then**
    for $m_2 = m_2^{\rm lb}(m_1) : (M-m_1)$ **do**
      Calculate the lower bound of t as $t^{\rm lb}=p_1^{\rm lb}+p_2^{\rm lb}$, and the upper bound of t as $t^{\rm ub}$ from (56). Use the one-dimensional search to find the optimal t that achieves the minimum objective value. Denote the optimal objective value $\bar{\varepsilon}_2(m_1, m_2)$.
    end
    Given m_1, find the blocklength m_2 with the minimum value of $\varepsilon_2(m_1, m_2)$:

$$m_2^{\#}\Big|_{m_1} = \mathop{\arg\min}_{m_2^{\rm lb}(m_1)\leq m_2 \leq M-m_1} \varepsilon_2(m_1, m_2).$$

  end
end
Return

$$m_1^\star = \mathop{\arg\min}_{m_1^{\rm lb}\leq m_1 \leq m_1^{\rm ub}} \varepsilon_2\left(m_1, m_2^{\#}\Big|_{m_1}\right), m_2^\star = m_2^{\#}\Big|_{m_1^\star}$$

and the corresponding $p_1^\star$ and $p_2^\star$.

IV. Extension to More Devices for the OMA Scheme

In this section, we consider the more general case when the system has more than two devices for the OMA scheme. The extension to other schemes will be studied in the future work.

A. Sytem Model and Problem Formulation

Let us denote the total number of devices as K, and the set of all devices as $\mathcal{K}$. We assume that the normalized channel gains of all K devices are arranged in a decreasing order, i.e., $h_1 > h_2 > \cdots > h_K$.[3] Then, we aim to jointly optimize the power and blocklength allocation to minimize the decoding error probability of the Kth device while guaranteeing the decoding error probability requirements of the first $K-1$ devices. Mathematically, the optimization problem can be formulated as follows:

$$\min_{\{m_k, k\in\mathcal{K}\}, \{p_k, k\in\mathcal{K}\}} \varepsilon_K \tag{58a}$$

$$\text{s.t. } \varepsilon_k \leq \varepsilon_k^{\max}, \quad k \in \mathcal{K}\backslash K, \tag{58b}$$

$$\sum\nolimits_{k\in\mathcal{K}} m_k p_k \leq E_{\rm tot}, \tag{58c}$$

$$\sum\nolimits_{k\in\mathcal{K}} m_k \leq M, \tag{58d}$$

$$m_k \in \mathbb{Z}, \quad k \in \mathcal{K}. \tag{58e}$$

In contrast to the case of two devices where the globally optimal solution to Problem (7) can be obtained, the globally optimal solution to Problem (58) for the more general case is

[3]Due to the small-scale fading, the probability that any two or more devices have the same channel gain is equal to zero.

not available. In the following, we aim to obtain a suboptimal solution to Problem (58).

B. Problem Reformulation

To make Problem (58) tractable, we again approximate V as one, i.e., $V \approx 1$. This approximation is very accurate when the SNR value γ is very high, i.e., $\gamma \gg 1$. As the decoding error probability is a decreasing function of power and blocklength, we can readily prove that constraints (58b), (58c) and (58d) hold with equality at the optimum point by using the contradiction method. By using the fact that $\varepsilon_k = \varepsilon_k^{\max}, k \in \mathcal{K}\backslash K$, p_k can be derived as a function of m_k, given by

$$p_k = \frac{2^{\frac{D}{m_k}+\frac{Q^{-1}(\varepsilon_k^{\max})}{\ln 2\sqrt{m_k}}}-1}{h_k} \triangleq \chi(m_k), k \in \mathcal{K}\backslash K. \quad (59)$$

By substituting (59) into (58), Problem (58) can be transformed as follows:

$$\min_{\{m_k,k\in\mathcal{K}\},p_K} \quad \varepsilon_K \quad (60a)$$

$$\text{s.t.} \ \sum\nolimits_{k\in\mathcal{K}\backslash K} m_k\chi(m_k) + m_K p_K = E_{\text{tot}}, \quad (60b)$$

$$\sum\nolimits_{k\in\mathcal{K}} m_k = M, m_k \in \mathbb{Z}, k \in \mathcal{K}. \quad (60c)$$

Compared with the original Problem (58), the number of optimization variables of Problem (60) is significantly reduced. However, this problem is still difficult to solve. In the following, we first use the exhaustive search to find m_K, and then optimize p_K. To this end, we need to find tight lower and upper bounds of m_K to reduce the computational complexity.

C. Bounds of m_K

In this subsection, we attempt to obtain the bounds of m_K. We first provide the following theorem.

Theorem 3: Define $A_k = Q^{-1}(\varepsilon_k^{\max})/\ln 2$ and $g(m_k) \triangleq m_k\chi(m_k)$. Then, $g(m_k)$ is a monotonically decreasing and convex function when m_k satisfies:

$$\sqrt{m_k} < \frac{\frac{3}{4}A_k \ln 2 + \sqrt{\frac{9}{16}(\ln 2)^2 A_k^2 + 8D\ln 2}}{2}. \quad (61)$$

Proof: Please see Appendix D. ∎

In general, for a typical URLLC system, the number of transmission bits is around 100 bits and the decoding error probability requirement is around 10^{-9}. Then, A_k is 8.653, and the value of the right hand side of (61) is given by 14.236. Then, when $m_k \leq 202$, the inequality (61) holds. In short packet transmission with OMA scheme, the number of blocklength to each device is generally smaller than 100. Hence, in our considered scenario, $g(m_k)$ can be regarded as a monotonically decreasing and convex function.

In the following, we provide an iterative procedure to obtain the tight bounds of m_K. Since $m_k p_k = g(m_k) < E_{\text{tot}}$ and $g(m_k)$ is a monotonically decreasing function, we can obtain the lower bound of m_k by using the bisection search method, which is denoted as $m_k^{\text{lb}(0)}, k \in \mathcal{K}\backslash K$. To guarantee the meaningfulness of ε_K, the following inequality holds

$$p_K > \left(2^{\frac{D}{m_K}}-1\right)/h_K. \quad (62)$$

Then, we have

$$E_{\text{tot}} > m_K p_K > \frac{m_K}{h_K}\left(2^{\frac{D}{m_K}}-1\right) \triangleq q(m_K). \quad (63)$$

As a result, we can obtain the lower bound of m_K from (63), which is denoted as $m_K^{\text{lb}(0)}$. Then, for each device k, the upper bound of m_k is given by $m_k^{\text{ub}(0)} = M - \sum_{i\in\mathcal{K}\backslash k} m_i^{\text{lb}(0)}$, $k \in \mathcal{K}$. Since $q(m_K)$ defined in (63) is a monotonically decreasing function, we have $q(m_K) > q(m_K^{\text{ub}(0)})$. In addition, $g(m_k)$ is a monotonically decreasing function of m_k, and we have $g(m_k) > g(m_k^{\text{ub}(0)}), k \in \mathcal{K}\backslash K$. Then, for each $k \in \mathcal{K}\backslash K$, we have

$$E_{\text{tot}} - \sum_{i\in\mathcal{K}\backslash\{K,k\}} g\left(m_i^{\text{ub}(0)}\right) - q\left(m_K^{\text{ub}(0)}\right) > g(m_k), k \in \mathcal{K}\backslash K. \quad (64)$$

Then, the lower bound of m_k for $k \in \mathcal{K}\backslash K$ can be obtained as $m_k^{\text{lb}(1)}, k \in \mathcal{K}\backslash K$. For the Kth device, we have

$$E_{\text{tot}} - \sum\nolimits_{k\in\mathcal{K}\backslash K} g(m_k^{\text{ub}(0)}) > \frac{m_K}{h_K}\left(2^{\frac{D}{m_K}}-1\right). \quad (65)$$

Then, based on (65) we can update the lower bound of m_K as $m_K^{\text{lb}(1)}$. Then, for each device k, the upper bound of m_k is given by $m_k^{\text{ub}(1)} = M - \sum_{i\in\mathcal{K}\backslash k} m_i^{\text{lb}(1)}, k \in \mathcal{K}$. Finally, repeat the above procedure until $m_K^{\text{lb}(n)} = m_K^{\text{lb}(n+1)}$ and $m_K^{\text{ub}(n)} = m_K^{\text{ub}(n+1)}$, where n is the iteration number. Similar to the case of two devices, the above procedure can be proved to be convergent, and denote the final converged upper and lower bounds of m_K as m_K^{ub} and m_K^{lb}, respectively.

D. Optimization of p_K With Given m_K

Given m_K, ε_K is a monotonically decreasing function of p_K and p_K is given by

$$p_K = \frac{1}{m_K}\left(E_{\text{tot}} - \sum\nolimits_{k\in\mathcal{K}\backslash K} m_k\chi(m_k)\right), \quad (66)$$

Problem (60) can then be equivalently transformed as

$$\min_{\{m_k,k\in\mathcal{K}\backslash K\}} \quad \sum\nolimits_{k\in\mathcal{K}\backslash K} m_k\chi(m_k) \quad (67a)$$

$$\text{s.t.} \ \sum\nolimits_{k\in\mathcal{K}\backslash K} m_k = M - m_K, \quad (67b)$$

$$m_k \in \mathbb{Z}, k \in \mathcal{K}\backslash K. \quad (67c)$$

This problem is still difficult to solve due to the integer constraint (67c). To resolve this issue, we relax $\{m_k, k \in \mathcal{K}\backslash K\}$ to continuous values. Then, Problem (67) can be relaxed as follows:

$$\min_{\{m_k,k\in\mathcal{K}\backslash K\}} \quad \sum_{k\in\mathcal{K}\backslash K} m_k\chi(m_k) \quad (68a)$$

$$\text{s.t.} \ m_k \geq m_k^{\text{lb}}, k \in \mathcal{K}\backslash K, (67b), \quad (68b)$$

where $\{m_k^{\text{lb}}, k \in \mathcal{K}\backslash K\}$ are given in the above subsection. Since $m_k\chi(m_k)$ is proved to be convex as shown in

Theorem 2, Problem (68) is a convex optimization problem, which can be solved by using the Lagrangian dual decomposition method [31]. We first introduce the Lagrange multiplier λ associated with constraint (67b), the partial Lagrangian function of Problem (68) is given by

$$\mathcal{L}(\mathbf{m},\lambda)=\sum_{k\in\mathcal{K}\backslash K} m_k\chi(m_k)+\lambda\left(\sum_{k\in\mathcal{K}\backslash K} m_k-M-m_K\right), \quad (69)$$

where $\mathbf{m}=\{m_k, k\in\mathcal{K}\backslash K\}$.

In the following, we aim to obtain the optimal m_k, $k\in\mathcal{K}\backslash K$ for given λ, which is denoted as $m_k^\star(\lambda), k\in\mathcal{K}\backslash K$. As $\mathcal{L}(\mathbf{m},\lambda)$ is a convex function of $m_k, k\in\mathcal{K}\backslash K$, the optimal m_k for given λ can be obtained in the following. If

$$\left.\frac{\partial\mathcal{L}(\mathbf{m},\lambda)}{\partial m_k}\right|_{m_k=m_k^{\mathrm{lb}}}\geq 0, \quad (70)$$

the optimal m_k is given by $m_k^\star(\lambda)=m_k^{\mathrm{lb}}$. Otherwise, $m_k^\star(\lambda)$ is the solution to the following equation:

$$\frac{\partial\mathcal{L}(\mathbf{m},\lambda)}{\partial m_k}=0, \quad (71)$$

which can be obtained by using the bisection search method.

Upon obtaining the optimal $m_k^\star(\lambda), k\in\mathcal{K}\backslash K$, we can obtain the value of the left hand side of (67b), which is defined as function $F(\lambda)$

$$F(\lambda)\triangleq\sum_{k\in\mathcal{K}\backslash K} m_k^\star(\lambda). \quad (72)$$

By using the similar technique as in Appendix A of [32], we can prove that $F(\lambda)$ is a monotonically decreasing function of λ. Hence, the bisection search method can be adopted to find the solution of λ to the equation $F(\lambda)=M-m_K$ if the original problem is feasible.

Denote the solution obtained by solving the relaxed problem (68) as $\{\bar{m}_k, k\in\mathcal{K}\backslash K\}$. In general, $\{\bar{m}_k, k\in\mathcal{K}\backslash K\}$ may violate the integer requirement. Hence, we need to convert the continuous $\{\bar{m}_k, k\in\mathcal{K}\backslash K\}$ to integer solutions, denoted as $\{m_k^\star, k\in\mathcal{K}\backslash K\}$. However, the integer conversion problem is a combinatorial optimization problem, which is NP to solve. In the following, we apply the greedy search method to solve the integer conversion problem. Specifically, we first initialize the integer solution as $m_k^\star=\lfloor\bar{m}_k\rfloor, k\in\mathcal{K}\backslash K$. Note that $g(m_k)$ is a monotonically decreasing function of m_k. Each time we allocate one blocklength to the device with the largest decrement of $g(m_k)$, i.e., $k^*=\arg\max_{k\in\mathcal{K}\backslash K}\{g(m_k)-g(m_k+1)\}$. The rational behind this is that based on (67b) more energy can be allocated to the Kth device, thus decreasing ε_K most. For the k^*th device, we set $m_{k^*}^\star=m_{k^*}^\star+1$. If $p_K^\star$ is smaller than zero, set $\varepsilon_K^\star=1$. Repeat the above procedure until $\sum_{k\in\mathcal{K}\backslash K} m_k^\star=M-m_K$. Then, the power allocated to the Kth device can be recalculated as

$$p_K=\frac{E_{\mathrm{tot}}-\sum_{k\in\mathcal{K}\backslash K} g(m_k^\star)}{m_K}. \quad (73)$$

Thus, we can calculate ε_K based on current m_K and $p_K^\star$.

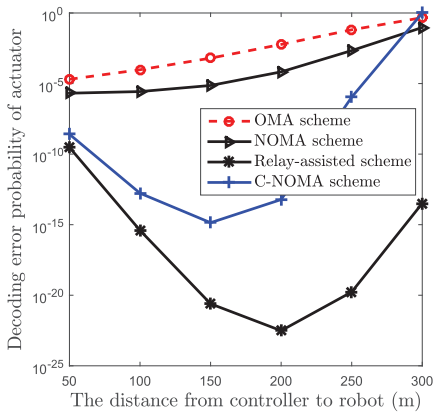

Fig. 2. The decoding error probability of the actuator versus the distance from the controller to the robot under four schemes, when $D=100$ bits, $M=100$ symbols, $\tilde{E}_{\mathrm{tot}}=5\times10^{-5}$ Joule.

V. Simulations Results

In this section, simulation results are provided to evaluate the performance of the proposed algorithms. For simplicity, we assume that the controller, the robot and the actuator are located on the same line, and the robot is moving from the controller to the actuator, and the robot is served as the relay to help the transmission of the actuator. The distance between the controller and the actuator is set as 500 m. Let us denote d_1, d_2 and d_3 as the distances from the controller to the robot, the controller to the actuator, and the robot to the actuator, respectively. The system bandwidth is set as $B=1$ MHz. Hence, the downlink transmission delay duration is calculated as 100 us that meets a criterion of industrial standards [13]. The noise power spectral density is -173 dBm/Hz. The decoding (packet) error probability requirement for the robot is set as 10^{-9}. The large-scale path loss model is $35.3+37.6\log_{10}\mathrm{dB}$ [33]. The simulation section is divided into two subsections. In the first subsection, we assume that the channel gain is only determined by the path loss in order to obtain the insights of all the schemes. In the second subsection, we consider the network availability performance [17] taking into account small-scale fading obeying the Rayleigh distribution.

A. Only Large-Scale Fading

In Fig. 2, we first study the impact of distance d_1 on the decoding error probability. We observe that relay-assisted transmission outperforms the other three schemes. It is interesting to see that when the robot moves from the controller to the actuator, the decoding error probability achieved by the OMA and NOMA schemes always decreases. The main reason is that the channel gain from controller to robot decreases with increasing the distance, so the energy and blocklength required for the robot to guarantee its error probability requirement increases. As a result, the available energy and blocklength for the actuator will decrease. On the other hand, the reliability performances achieved by the C-NOMA and relay-assisted schemes first increase and then decrease when the robot moves in the line. This can be explained as follows. When the

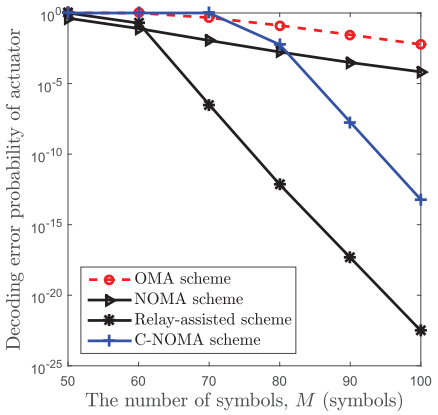

Fig. 3. The decoding error probability of the actuator versus the number of symbols under four schemes, when $D = 100$ bits, $\tilde{E}_{\rm tot} = 5 \times 10^{-5}$ Joule, $d_1 = 200$ m, $d_2 = 500$ m, and $d_3 = 300$ m.

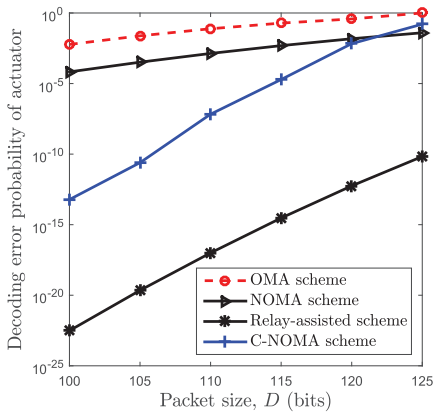

Fig. 4. The decoding error probability of the actuator versus packet size under four schemes, when $M = 100$ sysmbols, $\tilde{E}_{\rm tot} = 5 \times 10^{-5}$ Joule, $d_1 = 200$ m, $d_2 = 500$ m, and $d_3 = 300$ m.

robot moves from 50 m to 150 m for the C-NOMA and 200 m for relay-assisted scheme, the channel gain from the robot to the actuator becomes weak, which is the performance bottleneck that limits the decoding error probability of the actuator. However, when the robot continues to move towards the actuator, the transmission link from the controller to the robot becomes the bottleneck link. Hence, the distance d_1 can be optimized to additionally improve the system performance, which can be treated in the future work. It is interesting to observe that the C-NOMA performs worse than the relay-assisted scheme, which is due to the larger feasible region for the latter scheme as explained at the end of Section III.

In Fig. 3, we examine the impact of available blocklength M on the decoding error probability of the actuator. As expected, larger M leads to much better reliability performance in all schemes, and the decoding error probability achieved by the relay scheme decreases from 1 to 10^{-22} with M increasing from 50 to 100. It is interesting to find that when the blocklength M is equal to 50 and 60, the NOMA scheme has the best reliability performance since the whole transmission blocklength can be used for transmission in NOMA, while the whole blocklength should be divided into two parts for the other schemes. Importantly, this provides insights for the system designer that when the blocklength is very limited as in URLLC, relay may not be a good option since some blocklengths needs to be reserved for the two-stage transmission. However, further increasing M, the relay-assisted transmission and the C-NOMA start to perform better than the NOMA scheme, and the performance gain monotonically increases with M. However, the cross-point associated with the relay scheme is much lower than that of the C-NOMA scheme due to the shrinking feasible region associated with the latter scheme. Furthermore, the curves of both schemes have the same slope with different bias.

In Fig. 4, we study the impact of the packet size D on the decoding error probability. As expected, a larger packet size leads to a higher error probability for all schemes. The performance advantage of the relay-assisted scheme over the OMA and NOMA schemes shrinks with the increase of D. It is interesting to find that the curves associated with the

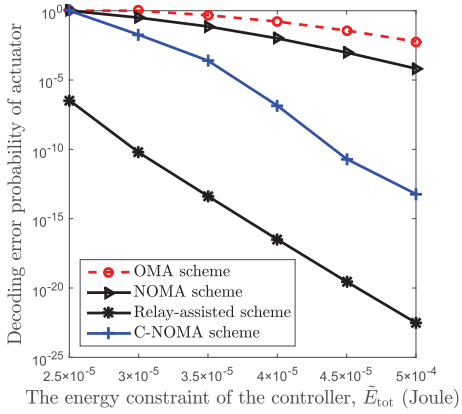

Fig. 5. The decoding error probability of the actuator versus the energy constraint under four schemes, when $D = 100$ bits, $M = 100$ symbols, $d_1 = 200$ m, $d_2 = 500$ m, and $d_3 = 300$ m.

OMA and NOMA schemes have almost the same slope, while those of the relay-assisted transmission and the C-NOMA scheme are similar. The main reason may be that the latter two schemes apply relay to assist the transmission. Similar to the observations in [24], the NOMA achieves better performance than the OMA scheme. When $D = 125$ bits, the C-NOMA is even worse than the NOMA since some blocklengths should be reserved for the two-stage transmission in the former scheme.

In Fig. 5, we study the impact of the total energy on the decoding error probability. It is observed that more available energy leads to better reliability performance as expected. It is also seen that the relay-assisted transmission has the best performance, and the performance gain increases with the amount of available energy. It is shown that with sufficient energy, transmission with the aid of relay (i.e., the relay-assisted transmission and the C-NOMA transmission) is beneficial for the system performance. When $\tilde{E}_{\rm tot} = 5 \times 10^{-5}$ Joule, the decoding error probability achieved by the relay-assisted transmission is extremely low.

In Fig. 6, we study the performance comparison between the OMA scheme in Section III and the general OMA in Section IV. Denote the number of devices as K. If $K = 2$, both the OMA scheme and the general OMA scheme

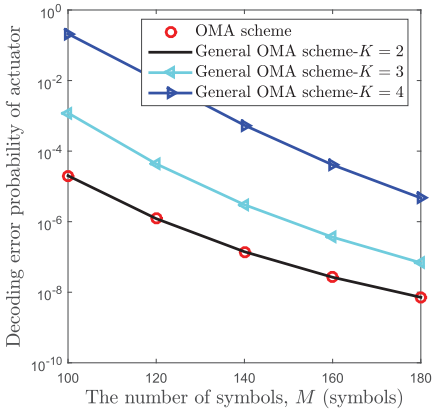

Fig. 6. The decoding error probability of the actuator versus the number of symbols for the OMA scheme the general OMA scheme, when $D = 100$ bits, and $\tilde{E}_{\rm tot} = 5 \times 10^{-5}$ Joule.

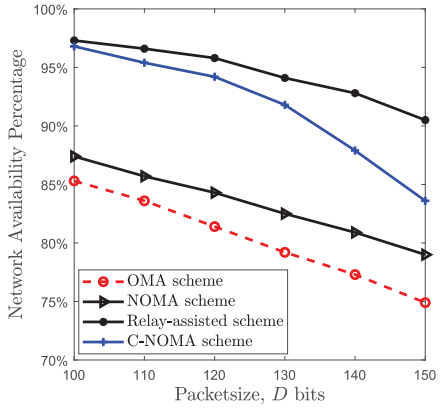

Fig. 7. The network availability percentage versus the packet size D under four schemes, when $\tilde{E}_{\rm tot} = 5 \times 10^{-4}$ Joule, $M = 100$ symbols.

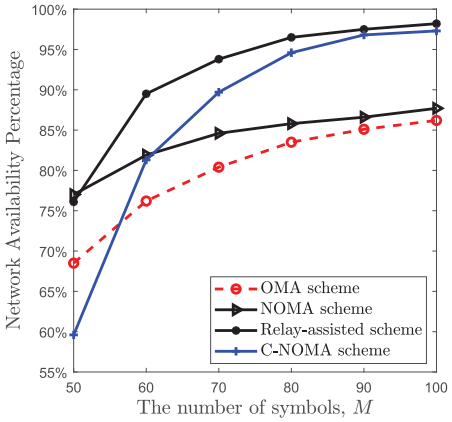

Fig. 8. The network availability percentage versus the number of symbols M under four schemes, when $\tilde{E}_{\rm tot} = 5 \times 10^{-4}$ Joule, $D = 100$ bits.

are applicable. However, for the case with $K > 2$, only the general OMA scheme is applicable. For the first $K-1$th devices, the distance of the kth device to the controller is set as $50 \times k$ m, while the distance of the last device to the controller is set as 500 m. The other parameters are the same as the previous figures. It is interesting to find that the decoding error probability achieved by the OMA scheme and the general OMA scheme is almost the same when $K = 2$, which implies that the general OMA can achieve almost the globally optimal solution in this setup. However, the general OMA scheme has lower complexity than the OMA scheme. It is also noted from this figure that the decoding error probability achieved by the Kth device increases when the number of total devices increases. This can be explained as follows. When the number of total devices increases, the total resource such as energy and channel blocklength allocated to the first $K-1$ devices will increase. Then, the left resource allocated for the Kth device decreases, leading to its worse decoding error probability performance.

B. Network Availability Performance (Channel Generation Times = 1000)

In this subsection, the small-scale fading channel is taken into consideration in the channel gain, and we study the network availability performance, which is defined as the ratio of the number of channel generations, where the decoding error probability achieved by both devices is no larger than 10^{-9}, to the total number of channel generations [2]. In the following simulations, the total number of channel generations is set as 1000. The distances are set as $d_1 = 200$ m, $d_2 = 500$ m, and $d_3 = 300$ m, respectively.

Fig. 7 illustrates the network availability performance versus the packet size D for all schemes. As expected, the network availability performance achieved by all schemes decreases with D. The relay-assisted transmission has the best network availability performance over the whole region of D. It is observed that when $D = 100$ bits, the network availability percentage of the relay-assisted scheme and the C-NOMA scheme is almost the same, as high as 98%. However, the performance gap of these two schemes increases rapidly with D due to the shrinking feasible region of the C-NOMA scheme compared to the relay-assisted transmission. However, the network availability performance for both the OMA scheme and the NOMA scheme are lower than that of relay-assisted scheme and C-NOMA scheme, and the network availability percentage is as low as 87% for NOMA scheme even when $D = 100$ bits.

Fig. 8 shows the network availability performance versus the number of symbols for four schemes. As expected, the network availability performance increases with M for all schemes. The NOMA scheme performs slightly better than the relay scheme when $M = 50$. It is interesting to note that the C-NOMA scheme has the worst performance when $M = 50$, which means that this scheme is not a good option when there is stringent latency requirement. However, the network availability percentage of the C-NOMA increases rapidly with M, and finally converges to almost the same value as that of the relay-assisted scheme, that is equal to 97% when $M = 100$. It is also noted that the OMA scheme converges to almost the same performance as that of the NOMA scheme, and is low (86% when $M = 100$). It is interesting to find that the network availability performance of all the schemes saturates in the high region of M, which indicates that the number of available blocklength is not necessary to be very large. This can be explained by using the result in [29]: The dispersion of quasi-static fading channels converges to

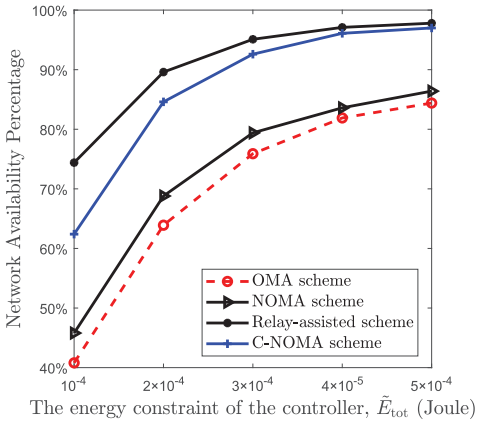

Fig. 9. The network availability percentage versus energy limit under four schemes, when $D = 100$ bits, $M = 100$ symbols.

zero, which implies that the maximum achievable data rate converges quickly to the outage capacity.

Finally, Fig. 9 depicts the network availability performance versus the energy limit $\tilde{E}_{\rm tot}$ for all schemes. As expected, the network performance achieved by all schemes increases with $\tilde{E}_{\rm tot}$. It is also observed that relay-assisted scheme has the best network availability performance. However, the performance gain over the C-NOMA scheme decreases with $\tilde{E}_{\rm tot}$ and both curves coincide in the high regime of $\tilde{E}_{\rm tot}$, where both schemes can achieve the network availability percentage of 98%. On the other hand, both the NOMA scheme and OMA scheme have very low network availability percentage, e.g., 86% when $\tilde{E}_{\rm tot} = 5 \times 10^{-4}$ Joule. The performance gap between the relay-assisted scheme and NOMA is significant, up to 30%.

VI. Conclusion

This work studied the resource allocation of short packet transmission for mission-critical IoT to achieve low latency and high reliability under fundamental transmission schemes, which include OMA, NOMA, relay-assisted transmission and C-NOMA transmission. We formulated an optimization problem to minimize the decoding error probability for the actuator with lower channel gain while guaranteeing that the robot achieved a low error probability target. To facilitate the optimal design of the blocklength and power allocation, we derived the tight bounds on the blocklength and the transmit power for all schemes. Simulation results demonstrated that relay-assisted transmission significantly outperforms the other schemes for most cases in terms of packet error probability as well as network availability percentage performance. It was also noted that the NOMA scheme performs well when the delay requirement is very stringent. For the C-NOMA and relay-assisted schemes, there exists one optimal transmission distance between the central controller and the robot. We also observed that the general OMA scheme can achieve almost the same performance as the OMA scheme, while the former scheme has a lower complexity.

Concerning our future work, we will consider a more general scenario with more than two devices for the other three schemes.

Appendix A
Proof of Lemma 1

We prove it by using contradiction. In the following, we first prove that constraint (7b) holds with equality at the optimum solution. The second one can be proved similarly.

Denote the optimal solution of Problem (7) as $\mathbf{s}^\star = \{m_1^\star, m_2^\star, p_1^\star, p_2^\star\}$ and the corresponding ε_1 and ε_2 are denoted as $\varepsilon_1^\star$ and $\varepsilon_2^\star$, respectively. Suppose that $\varepsilon_1^\star$ is strictly smaller than $\varepsilon_1^{\max}$, i.e., $\varepsilon_1^\star < \varepsilon_1^{\max}$. In Proposition 1 of [24], the author proved that $Q\left(f\left(\gamma_1, m_1, D\right)\right)$ monotonically decreases with γ_1. Then, we can construct a new solution $\mathbf{s}^\# = \{m_1^\star, m_2^\star, p_1^\#, p_2^\#\}$, where $p_1^\# = p_1^\star - \Delta p$ and $p_2^\# = p_2^\star + \frac{m_1^\star \Delta p}{m_2^\star}$ with $\Delta p > 0$. It can be verified that the following equation holds,

$$m_1^\star p_1^\# + m_2^\star p_2^\# = m_1^\star p_1^\star + m_2^\star p_2^\star \le E_{\rm tot}. \tag{74}$$

Hence, the new constructed solution $\mathbf{s}^\#$ still satisfies the energy constraint (7c). In addition, we can always find a proper positive Δp such that the new $\varepsilon_1^\#$ with the new solution $\mathbf{s}^\#$ is equal to $\varepsilon_1^{\max}$, i.e., $\varepsilon_1^\# = \varepsilon_1^{\max}$, which satisfies constraint (7b). Hence, the new constructed solution $\mathbf{s}^\#$ is a feasible solution of Problem (7). Since $p_2^\# > p_2^\star$, we have $\varepsilon_2^\# < \varepsilon_2^\star$. This contradicts with the assumption that $\mathbf{s}^\star$ is an optimal solution. The same method is applicable to the proof of the second conclusion.

Appendix B
Proof of Theorem 1

The first and second derivative of function $\tilde{g}(m_2)$ w.r.t. m_2 can be calculated as

$$\tilde{g}'(m_2) = \frac{1}{2\ln 2}\frac{1}{\sqrt{m_2}}\ln\left(1+\frac{E_2h_2}{m_2}\right) - \frac{1}{\ln 2}\frac{1}{\sqrt{m_2}}\frac{E_2h_2}{m_2+E_2h_2} + \frac{D}{2}m_2^{-\frac{3}{2}} \tag{75}$$

$$\tilde{g}''(m_2) = \underbrace{-\frac{1}{4\ln 2}\frac{\ln\left(1+\frac{E_2h_2}{m_2}\right)}{m_2\sqrt{m_2}} + \frac{E_2h_2}{\ln 2\sqrt{m_2}(m_2+E_2h_2)^2}}_{?} \underbrace{-\frac{3}{4}Dm_2^{-\frac{5}{2}}}_{<0}. \tag{76}$$

Obviously, the last term of $g''(m_2)$ is negative, we only need to prove that the sum of the first two terms is negative under the condition of $\frac{E_2h_2}{M-m_1} \ge e-1$.

Since $m_2^{\rm lb} \le m_2 \le M - m_1$, we have

$$\frac{E_2h_2}{m_2} \ge \frac{E_2h_2}{M-m_1} \ge e-1. \tag{77}$$

Then, the following inequality follows:

$$4 \le \left(\frac{E_2h_2}{m_2} + 2 + \frac{m_2}{E_2h_2}\right)\ln\left(1+\frac{E_2h_2}{m_2}\right). \tag{78}$$

By rearranging the terms of the above inequality, we can prove that the sum of the first two terms is negative, which completes the proof.

APPENDIX C
PROOF OF THEOREM 2

We prove this theorem by using the method of contradiction. Denote the optimal p_1 of Problem (28) as $p_1^\star$ and the corresponding decoding error probability is given by $\bar{\varepsilon}_1(p_1^\star)$. Suppose that $\bar{\varepsilon}_1(p_1^\star)$ is strictly less than $\varepsilon_1^{\max}$, i.e., $\bar{\varepsilon}_1(p_1^\star) < \varepsilon_1^{\max}$. Since $\hat{\varepsilon}_1(p_1^{\rm lb}) > \varepsilon_1(p_1^{\rm lb})$, we have

$$\begin{aligned}\bar{\varepsilon}_1(p_1^{\rm lb}) &= \varepsilon_1(p_1^{\rm lb}) + (\hat{\varepsilon}_1(p_1^{\rm lb}) - \varepsilon_1(p_1^{\rm lb}))\varepsilon_2^1(p_1^{\rm lb}) \\ &= \varepsilon_1^{\max} + (\hat{\varepsilon}_1(p_1^{\rm lb}) - \varepsilon_1(p_1^{\rm lb}))\varepsilon_2^1(p_1^{\rm lb}) > \varepsilon_1^{\max}, \quad (79)\end{aligned}$$

where $\varepsilon_1(p_1^{\rm lb}) = \varepsilon_1^{\max}$ is used in the second equality. As $\bar{\varepsilon}_1(p_1)$ is a continuous function, there must exist a value $p_1^{\&}$ within the range of $p_1^{\rm lb} < p_1^{\&} < p_1^\star$ such that $\bar{\varepsilon}_1(p_1^{\&}) = \varepsilon_1^{\max}$. On the other hand, the objective value $\varepsilon_2(p_1)$ is a monotonically increasing function of p_1 since $p_2 = E_{\rm tot}/m - p_1$. Hence, we have $\varepsilon_2(p_1^{\&}) < \varepsilon_2(p_1^\star)$, which contradicts the assumption that $p_1^\star$ is an optimal solution.

APPENDIX D
PROOF OF THEOREM 3

We first prove its convexity. Define function

$$J(m_k) \triangleq m_k 2^{\frac{D}{m_k} + \frac{A_k}{\sqrt{m_k}}}. \quad (80)$$

Then, $g(m_k)$ can be rewritten as $g(m_k) = (J(m_k) - m_k)/h_k$. Then, if $J(m_k)$ is convex, function $g(m_k)$ is also convex. Hence, in the following, we prove that $J(m_k)$ is a convex function. Define function $\tilde{J}(m_k)$ as

$$\tilde{J}(m_k) \triangleq \ln\left(J(m_k)\right) = \ln(m_k) + \left(\frac{D}{m_k} + \frac{A_k}{\sqrt{m_k}}\right)\ln 2. \quad (81)$$

The second-order derivative of $\tilde{J}(m_k)$ w.r.t. m_k is given by

$$\tilde{J}''(m_k) = \frac{1}{m_k^3}\left(2D\ln 2 - m_k + \frac{3}{4}A_k\sqrt{m_k}\ln 2\right). \quad (82)$$

Note that the denominator of (82) is a quadratic function of $\sqrt{m_k}$. Hence, if the inequality in (61) is satisfied, $\tilde{J}''(m_k)$ is always positive, which means $\tilde{J}(m_k)$ is a convex function of m_k. Since $J(m_k) = e^{\tilde{J}(m_k)}$, according to the composition rule in [31], we can show that $J(m_k)$ is also a convex function. Hence, $g(m_k)$ is a convex function of m_k when the inequality in (61) is satisfied.

Now, we proceed to prove that $g(m_k)$ is a monotonically decreasing function of m_k. The first-order derivative of $g(m_k)$ w.r.t. m_k is given by

$$g'(m_k) = \frac{1}{h_k}\left[2^{\frac{D}{m_k} + \frac{A_k}{\sqrt{m_k}}}\left(-\frac{D}{m_k}\ln 2 - \frac{\ln 2}{2}\frac{A_k}{\sqrt{m_k}} + 1\right) - 1\right]. \quad (83)$$

Since $g(m_k)$ is a convex function, we have $g''(m_k) \geq 0$, which means $g'(m_k)$ is a monotonically increasing function. Hence, we have

$$g'(m_k) < g'(\infty) = 0. \quad (84)$$

Hence, $g(m_k)$ is a monotonically decreasing function of m_k when the inequality in (61) holds.

ACKNOWLEDGMENT

The author A. Nallanathan, would like to thank the U.K. Engineering and the Physical Sciences Research Council under Grant EP/N029666/1.

REFERENCES

[1] M. Shafi *et al.*, "5G: A tutorial overview of standards, trials, challenges, deployment, and practice," *IEEE J. Sel. Areas Commun.*, vol. 35, no. 6, pp. 1201–1221, Jun. 2017.
[2] P. Schulz *et al.*, "Latency critical IoT applications in 5G: Perspective on the design of radio interface and network architecture," *IEEE Commun. Mag.*, vol. 55, no. 2, pp. 70–78, Feb. 2017.
[3] M. Bennis, M. Debbah, and H. V. Poor, "Ultrareliable and low-latency wireless communication: Tail, risk, and scale," *Proc. IEEE*, vol. 106, no. 10, pp. 1834–1853, Oct. 2018.
[4] P. Popovski *et al.*, "Wireless access for ultra-reliable low-latency communication (URLLC): Principles and building blocks," 2017, *arXiv:1708.07862*. [Online]. Available: https://arxiv.org/abs/1708.07862
[5] C. She, C. Yang, and T. Q. S. Quek, "Radio resource management for ultra-reliable and low-latency communications," *IEEE Commun. Mag.*, vol. 55, no. 6, pp. 72–78, Jun. 2017.
[6] J. J. Nielsen, R. Liu, and P. Popovski, "Ultra-reliable low latency communication using interface diversity," *IEEE Trans. Commun.*, vol. 66, no. 3, pp. 1322–1334, Mar. 2018.
[7] M. Mozaffari, W. Saad, M. Bennis, Y.-H. Nam, and M. Debbah, "A tutorial on UAVs for wireless networks: Applications, challenges, and open problems," *IEEE Commun. Surveys Tuts.*, vol. 21, no. 3, pp. 2334–2360, 3rd, Quart. 2019.
[8] M. Simsek, A. Aijaz, M. Dohler, J. Sachs, and G. Fettweis, "5G-enabled tactile Internet," *IEEE J. Sel. Areas Commun.*, vol. 34, no. 3, pp. 460–473, Mar. 2016.
[9] H. Ren *et al.*, "Power- and rate-adaptation improves the effective capacity of C-RAN for Nakagami- m fading channels," *IEEE Trans. Veh. Technol.*, vol. 67, no. 11, pp. 10841–10855, Nov. 2018.
[10] H. Ren *et al.*, "Low-latency C-RAN: An next-generation wireless approach," *IEEE Veh. Technol. Mag.*, vol. 13, no. 2, pp. 48–56, Jun. 2018.
[11] A. Varghese and D. Tandur, "Wireless requirements and challenges in Industry 4.0," in *Proc. IC3I*, Nov. 2014, pp. 634–638.
[12] L. Liu and W. Yu, "A D2D-based protocol for ultra-reliable wireless communications for industrial automation," *IEEE Trans. Wireless Commun.*, vol. 17, no. 8, pp. 5045–5058, Aug. 2018.
[13] O. N. C. Yilmaz, Y.-P. E. Wang, N. A. Johansson, N. Brahmi, S. A. Ashraf, and J. Sachs, "Analysis of ultra-reliable and low-latency 5G communication for a factory automation use case," in *Proc. IEEE Int. Conf. Commun. Workshop (ICCW)*, Jun. 2015, pp. 1190–1195.
[14] G. Durisi, T. Koch, and P. Popovski, "Toward massive, ultrareliable, and low-latency wireless communication with short packets," *Proc. IEEE*, vol. 104, no. 9, pp. 1711–1726, Aug. 2016.
[15] Y. Polyanskiy, H. V. Poor, and S. Verdú, "Channel coding rate in the finite blocklength regime," *IEEE Trans. Inf. Theory*, vol. 56, no. 5, pp. 2307–2359, May 2010.
[16] K. F. Trillingsgaard and P. Popovski, "Downlink transmission of short packets: Framing and control information revisited," *IEEE Trans. Commun.*, vol. 65, no. 5, pp. 2048–2061, May 2017.
[17] C. She, Z. Chen, C. Yang, T. Q. S. Quek, Y. Li, and B. Vucetic, "Improving network availability of ultra-reliable and low-latency communications with multi-connectivity," *IEEE Trans. Commun.*, vol. 66, no. 11, pp. 5482–5496, Nov. 2018.
[18] J. Östman, G. Durisi, E. G. Ström, M. C. Coskun, and G. Liva, "Short packets over block-memoryless fading channels: Pilot-assisted or Noncoherent transmission?" *IEEE Trans. Commun.*, vol. 67, no. 2, pp. 1521–1536, Feb. 2019.
[19] Y. Hu, J. Gross, and A. Schmeink, "On the capacity of relaying with finite blocklength," *IEEE Trans. Veh. Technol.*, vol. 65, no. 3, pp. 1790–1794, Mar. 2016.
[20] Y. Hu, A. Schmeink, and J. Gross, "Blocklength-limited performance of relaying under quasi-static Rayleigh channels," *IEEE Trans. Wireless Commun.*, vol. 15, no. 7, pp. 4548–4558, Jul. 2016.
[21] Y. Gu, H. Chen, Y. Li, L. Song, and B. Vucetic, "Short-packet two-way amplify-and-forward relaying," *IEEE Signal Process. Lett.*, vol. 25, no. 2, pp. 263–267, Feb. 2018.

[22] O. L. A. López, R. D. Souza, H. Alves, and E. M. G. Fernández, "Ultra reliable short message relaying with wireless power transfer," in *Proc. ICC*, May 2017, pp. 1–6.
[23] Y. Hu, M. C. Gursoy, and A. Schmeink, "Efficient transmission schemes for low-latency networks: NOMA vs. relaying," in *Proc. IEEE PIMRC*, Oct. 2017, pp. 1–6.
[24] X. Sun, S. Yan, N. Yang, Z. Ding, C. Shen, and Z. Zhong, "Short-packet downlink transmission with non-orthogonal multiple access," *IEEE Trans. Wireless Commun.*, vol. 17, no. 7, pp. 4550–4564, Jul. 2018.
[25] C. She, C. Yang, and T. Q. S. Quek, "Joint uplink and downlink resource configuration for ultra-reliable and low-latency communications," *IEEE Trans. Commun.*, vol. 66, no. 5, pp. 2266–2280, May 2018.
[26] Y. Hu, Y. Zhu, M. C. Gursoy, and A. Schmeink, "SWIPT-enabled relaying in IoT networks operating with finite blocklength codes," *IEEE J. Sel. Areas Commun.*, vol. 37, no. 1, pp. 74–88, Jan. 2018.
[27] C. Pan, H. Ren, Y. Deng, M. Elkashlan, and A. Nallanathan, "Joint blocklength and location optimization for URLLC-enabled UAV relay systems," *IEEE Commun. Lett.*, vol. 23, no. 3, pp. 498–501, Mar. 2019.
[28] C. E. Shannon, "A mathematical theory of communication," *Bell Syst. Tech. J.*, vol. 27, no. 3, pp. 379–423, Jul. 1948.
[29] W. Yang, G. Durisi, T. Koch, and Y. Polyanskiy, "Quasi-static multiple-antenna fading channels at finite blocklength," *IEEE Trans. Inf. Theory*, vol. 60, no. 7, pp. 4232–4265, Jun. 2014.
[30] Y. Liu, Z. Ding, M. Elkashlan, and H. V. Poor, "Cooperative non-orthogonal multiple access with simultaneous wireless information and power transfer," *IEEE J. Sel. Areas Commun.*, vol. 34, no. 4, pp. 938–953, Apr. 2016.
[31] S. Boyd and L. Vandenberghe, "Convex Optimization," Cambridge, U.K.: Cambridge Univ. Press, 2004.
[32] C. Pan *et al.*, "Intelligent reflecting surface aided MIMO broadcasting for simultaneous wireless information and power transfer," 2019, *arXiv:1908.04863*. [Online]. Available: https://arxiv.org/abs/1908.04863
[33] *Further Advancements for E-UTRA Physical Layer Aspects*, document 3GPP TR 36.814, E. U. T. R. Access, 2010.

Hong Ren received the B.S. degree in electrical engineering from Southwest Jiaotong University, Chengdu, China, in 2011, and the M.S. and Ph.D. degrees in electrical engineering from Southeast University, Nanjing, China, in 2014 and 2018, respectively. From October 2016 to January 2018, she was a Visiting Student with the School of Electronics and Computer Science, University of Southampton, U.K. She is currently a Post-Doctoral Scholar at the School of Electronic Engineering and Computer Science, Queen Mary University of London, U.K. Her research interests lie in the areas of communication and signal processing, including cooperative transmission, the Internet of Things and ultrareliability, and low latency communications.

Cunhua Pan received the B.S. and Ph.D. degrees from the School of Information Science and Engineering, Southeast University, Nanjing, China, in 2010 and 2015, respectively. From 2015 to 2016, he was a Research Associate at the University of Kent, U.K.

He held a postdoctoral position at the Queen Mary University of London, U.K., from 2016 and 2019, where he is currently a Lecturer (Assistant Professor). His research interests mainly include ultradense C-RAN, machine learning, UAV, the Internet of Things, and mobile edge computing. He serves as a TPC member for numerous conferences, such as ICC and GLOBECOM, and the Student Travel Grant Chair for ICC 2019. He also serves as an Editor for IEEE ACCESS.

Yansha Deng (S'13–M'19) received the Ph.D. degree in electrical engineering from the Queen Mary University of London, U.K., in 2015. From 2015 to 2017, she was a Post-Doctoral Research Fellow with King's College London, U.K., where she is currently a Lecturer (Assistant Professor) with the Department of Informatics. Her research interests include molecular communication, machine learning, and 5G wireless networks. She has also served as a TPC member for many IEEE conferences, such as IEEE GLOBECOM and ICC. She was a recipient of the Best Paper Awards from ICC 2016 and Globecom 2017 as the first author. She is currently an Associate Editor of the IEEE TRANSACTIONS ON COMMUNICATIONS, the IEEE TRANSACTIONS ON MOLECULAR, BIOLOGICAL AND MULTI-SCALE COMMUNICATIONS, and the Senior Editor of the IEEE COMMUNICATION LETTERS. She also received the Exemplary Reviewers of the IEEE TRANSACTIONS ON COMMUNICATIONS in 2016 and 2017, respectively, and the IEEE TRANSACTIONS ON WIRELESS COMMUNICATIONS in 2018.

Maged Elkashlan received the Ph.D. degree in electrical engineering from The University of British Columbia, Canada, in 2006. From 2007 to 2011, he was with the Commonwealth Scientific and Industrial Research Organization (CSIRO), Australia. During this time, he held visiting appointments at the University of New South Wales and University of Technology Sydney. In 2011, he joined the School of Electronic Engineering and Computer Science, Queen Mary University of London, U.K. His research interests fall into the broad areas of communication theory and statistical signal processing. He received the Best Paper Awards at the IEEE International Conference on Communications (ICC) in 2016 and 2014, respectively, the International Conference on Communications and Networking in China (CHINACOM) in 2014, and the IEEE Vehicular Technology Conference (VTC-Spring) in 2013. He currently serves as an Editor of the IEEE TRANSACTIONS ON WIRELESS COMMUNICATIONS and the IEEE TRANSACTIONS ON VEHICULAR TECHNOLOGY.

Arumugam Nallanathan (S'97–M'00–SM'05–F'17) has been a Professor of wireless communications and the Head of the Communication Systems Research (CSR) Group, School of Electronic Engineering and Computer Science, Queen Mary University of London, since September 2017. He was with the Department of Informatics, King's College London, from December 2007 to August 2017, where he was a Professor of wireless communications from April 2013 to August 2017, and a Visiting Professor from September 2017. He was an Assistant Professor with the Department of Electrical and Computer Engineering, National University of Singapore, from August 2000 to December 2007. His research interests include artificial intelligence for wireless systems, beyond 5G wireless networks, the Internet of Things (IoT), and molecular communications. He has published nearly 500 technical articles in scientific journals and international conferences.

Dr. Nallanathan is a co-recipient of the Best Paper Awards presented at the IEEE International Conference on Communications 2016 (ICC'2016), the IEEE Global Communications Conference 2017 (GLOBECOM'2017), and the IEEE Vehicular Technology Conference 2018 (VTC'2018). He has served as the Chair for the Signal Processing and Communication Electronics Technical Committee of the IEEE Communications Society and Technical Program Chair, and a member of the Technical Program Committees in numerous IEEE conferences. He received the IEEE Communications Society SPCE Outstanding Service Award 2012, and the IEEE Communications Society RCC Outstanding Service Award 2014. He was an Editor of the IEEE TRANSACTIONS ON WIRELESS COMMUNICATIONS (2006–2011), the IEEE TRANSACTIONS ON VEHICULAR TECHNOLOGY (2006–2017), the IEEE WIRELESS COMMUNICATIONS LETTERS, and the IEEE SIGNAL PROCESSING LETTERS. He is an Editor of the IEEE TRANSACTIONS ON COMMUNICATIONS. He is an IEEE Distinguished Lecturer. He has been selected as a Web of Science Highly Cited Researcher in 2016.